

ไมเซลล์เชื่อมขวางเตรียมจากแอมฟิฟิลิกโคพอลิเมอร์ที่มีหมู่แอกทีฟเอสเทอร์



บทคัดย่อและแฟ้มข้อมูลฉบับเต็มของวิทยานิพนธ์ตั้งแต่ปีการศึกษา 2554 ที่ให้บริการในคลังปัญญาจุฬาฯ (CUIR)
เป็นแฟ้มข้อมูลของนิสิตเจ้าของวิทยานิพนธ์ ที่ส่งผ่านทางบัณฑิตวิทยาลัย

The abstract and full text of theses from the academic year 2011 in Chulalongkorn University Intellectual Repository (CUIR)
are the thesis authors' files submitted through the University Graduate School.

วิทยานิพนธ์นี้เป็นส่วนหนึ่งของการศึกษาตามหลักสูตรปริญญาวิทยาศาสตรมหาบัณฑิต
สาขาวิชาเคมี ภาควิชาเคมี
คณะวิทยาศาสตร์ จุฬาลงกรณ์มหาวิทยาลัย
ปีการศึกษา 2559
ลิขสิทธิ์ของจุฬาลงกรณ์มหาวิทยาลัย

CROSS-LINKED MICELLES PREPARED FROM AMPHIPHILIC COPOLYMERS HAVING ACTIVE
ESTER GROUPS



A Thesis Submitted in Partial Fulfillment of the Requirements
for the Degree of Master of Science Program in Chemistry

Department of Chemistry

Faculty of Science

Chulalongkorn University

Academic Year 2016

Copyright of Chulalongkorn University

สุลิตา โนรี : ไมเซลล์เชื่อมขวางเตรียมจากแอมฟิฟิลิกโคพอลิเมอร์ที่มีหมู่แอคทีฟเอสเทอร์ (CROSS-LINKED MICELLES PREPARED FROM AMPHIPHILIC COPOLYMERS HAVING ACTIVE ESTER GROUPS) อ.ที่ปรึกษาวิทยานิพนธ์หลัก: ผศ. ดร.วราวุฒิ ตั้งพสุธาตล, อ.ที่ปรึกษาวิทยานิพนธ์ร่วม: รศ. ดร.วรวิรุ โสเวน, 55 หน้า.

พอลิ(เพนตะฟลูออโรฟีนิลเมทาคริเลต) ถูกเริ่มนำมาปรับปรุงผ่านการตัดแปรรหลังปฏิกิริยาพอลิเมอไรเซชันด้วยไอลิโกเอทิลีน ไกลคอลเอมีน เพื่อให้ได้ผลิตภัณฑ์เป็นโคพอลิเมอร์ระหว่างพอลิ(เพนตะฟลูออโรฟีนิลเมทาคริเลต) และพอลิ(ไอลิโกเอทิลีน ไกลคอล)เมทาคริลาไมด์ ซึ่งแอมฟิฟิลิกโคพอลิเมอร์แบบสุ่มชนิดนี้สามารถประกอบตัวเองในน้ำเพื่อเตรียมเป็นอนุภาคไมเซลล์ขนาดต่ำกว่า 100 นาโนเมตรโดย สามารถทำปฏิกิริยาแบบต่อเนื่องระหว่างหมู่เพนตะฟลูออโรฟีนิลและซิสตามีนซึ่งเป็นการเชื่อมขวางที่ประกอบไปด้วยไดไทออลเพื่อผลิตเป็นนาโนเจลที่ตอบสนองต่อปฏิกิริยารีดอกซ์ ส่วนหมู่เพนตะฟลูออโรฟีนิลที่เหลืออยู่สามารถกำจัดออกด้วยการทำปฏิกิริยากับไอโซโพรพิลามีนเพื่อผลิตเป็นระบบขนส่งยาที่ไม่เป็นพิษต่อเซลล์ ทุกขั้นตอนของการตัดแปรรหลังปฏิกิริยาพอลิเมอไรเซชันสามารถตรวจสอบได้ด้วยเทคนิค FTIR และ ฟลูออรีนเอ็นเอ็มอาร์ นอกจากนี้การปลดปล่อยโมเลกุลที่ไม่ชอบน้ำ ได้แก่ ไนล์เรดหรือเคอร์คูมิน ที่กักเก็บอยู่ภายในนาโนเจลสามารถถูกเร่งได้ในสภาวะที่มีกลูตาไทโอน ซึ่งจากผลการศึกษาความเข้ากันได้ของเซลล์และการนำเข้าสู่เซลล์แสดงให้เห็นว่านาโนเจลที่ตอบสนองต่อปฏิกิริยารีดอกซ์ที่เตรียมขึ้นได้นั้นมีคุณสมบัติที่เหมาะสมแก่การนำมาประยุกต์ใช้ทางด้านการขนานส่งยา



ภาควิชา เคมี
สาขาวิชา เคมี
ปีการศึกษา 2559

ลายมือชื่อนิสิต
ลายมือชื่อ อ.ที่ปรึกษาหลัก
ลายมือชื่อ อ.ที่ปรึกษาร่วม

5672126223 : MAJOR CHEMISTRY

KEYWORDS: POST-POLYMERIZATION MODIFICATION / PENTAFLUOROPHENYL ESTER / NANOGEL / DRUG CARRIER / ACTIVE ESTER GROUP / GLUTATHIONE / REDOX RESPONSIVE

SUSITA NOREE: CROSS-LINKED MICELLES PREPARED FROM AMPHIPHILIC COPOLYMERS HAVING ACTIVE ESTER GROUPS. ADVISOR: ASST. PROF. VARAWUT TANGPASUTHADOL, Ph.D., CO-ADVISOR: ASSOC. PROF. VORAVEE HOVEN, Ph.D., 55 pp.

Poly(pentafluorophenyl methacrylate) (PPFPMA) was first subjected to post-polymerization modification with oligo(ethylene glycol) methyl ether amine (OEG-NH₂) and yielded poly(pentafluorophenyl methacrylate)-co-poly(oligo(ethylene glycol methacrylamide)), PPFPMA-co-POEGMAM. These amphiphilic random copolymers can self-assemble into micellar nanoparticles in water having size less than 100 nm. By tandemly reacting the pentafluorophenyl (PFP) groups in the copolymeric nanoparticles with a dithiol crosslinker, cystamine, redox-responsive nanogels can be formed. The remaining PFP groups in the nanogels were removed by reacting with isopropylamine, resulting in a crosslinked drug delivery nano-carriers with highly biocompatible property. All stepwise post functionalization was monitored by FTIR and ¹⁹F NMR spectroscopy. Release of a hydrophobic guest molecules, Nile red (NR) or curcumin (CUR) from the nanogels, simultaneously encapsulated during micelles formation, can be accelerated in the presence of glutathione (GSH). Results from cytocompatibility evaluation and cellular uptake study suggested that these developed redox-responsive nanogels strongly possessed a potential for applications in controlled delivery.

Department: Chemistry

Student's Signature

Field of Study: Chemistry

Advisor's Signature

Academic Year: 2016

Co-Advisor's Signature

ACKNOWLEDGEMENTS

First of all, I would like to express my sincere and deep gratitude to my advisor, Assistant Professor Dr. Varawut Tangpasuthadol and my co-advisor, Associate Professor Dr. Voravee P. Hoven for their thoughtful guidance, steady encouragement and support, and consistent generosity and consideration. Working with them has been the best course of my study. I am sincerely grateful to all my committee members, Associate Professor Dr. Vudhichai Parasuk, Assistant Dr. Panuwat Padungros, and Associate Professor Dr. Panya Sunintaboon for their valuable suggestions and time to review my thesis.

My thanks also go to Ms. Songchan Puthong from the Institute of Biotechnology and Genetic Engineering, Chulalongkorn University for her excellent assistance and suggestions on cell culture studies.

Financial support for this work was provided by Thailand Research Fund (RSA5980071). SN acknowledges the Science Achievement Scholarship of Thailand, (SAST) for a M.Sc. scholarship and research assistantship scholarship for graduate students from Faculty of Science, Chulalongkorn University (Sci Super II) and Chulalongkorn University (Ratchadapisek Sompoj Endowment Fund).

Moreover, I wish to thank all members of VH and VT groups in Organic Synthesis Research Unit (OSRU) of Chulalongkorn University for their friendliness, helpful discussions, cheerful attitude and encouragements during my thesis work. Finally, I also wish to especially thank my family members for their love, kindness, and, support throughout my entire study.

CONTENTS

	Page
THAI ABSTRACT	iv
ENGLISH ABSTRACT	v
ACKNOWLEDGEMENTS	vi
CONTENTS	vii
LIST OF FIGURES	x
LIST OF TABLES	xiii
LIST OF SCHEMES	xiv
LIST OF ABBREVIATION.....	xv
CHAPTER I INTRODUCTION.....	1
1.1 Introduction	1
1.2 Objectives	9
1.3 Scope of investigation.....	9
CHAPTER II MATERIALS AND METHODS	11
2.1 Materials.....	11
2.2 Instrumentations.....	11
2.3 Experimental Procedure	12
2.3.1 Synthesis of pentafluorophenyl methacrylate.....	12
2.3.2 Synthesis of homopolymer by RAFT polymerization.....	13
2.3.2.1 Synthesis of poly(pentafluorophenyl methacrylate) (PPFPMA).....	13
2.3.2.2 Synthesis of poly(oligo(ethylene glycol) methacrylate) (POEGMA)...	13
2.3.3 Preparation of poly(oligo(ethylene glycol) methacrylate)-co- poly(pentafluorophenyl methacrylate) (POEGMA-co-PPFPMA) copolymer.....	13

2.3.3.1 Synthesis of random copolymer of poly(oligo(ethylene glycol) methacrylate)- <i>ran</i> -poly(pentafluorophenyl methacrylate) (POEGMA- <i>r</i> -PPFPMA).....	13
2.3.3.2 Synthesis of block copolymer of poly(pentafluorophenyl methacrylate)- <i>block</i> -poly(oligo(ethylene glycol) methacrylate) (PPFPMA- <i>b</i> -POEGMA).....	14
2.3.4 Synthesis of oligo(ethylene glycol) methyl ether amine (OEG-NH ₂)....	14
2.3.5 Post-polymerization modification of PPFPMA with OEG-NH ₂	15
2.3.6 Critical micelle concentration (CMC)	16
2.3.7 Preparation of hydrophobic molecule-loaded nanogels	16
2.3.7.1 Preparation of NR-loaded nanogels.....	16
2.3.7.2 Preparation of CUR-loaded nanogels	16
2.3.8 Post functionalization of NR-loaded nanogels	17
2.3.9 Redox-responsive release studies	17
2.3.9.1 Redox-responsive release of NR.....	17
2.3.9.2 Redox-responsive release of CUR	17
2.3.10 Cytocompatibility tests.....	18
2.3.10.1 Cytocompatibility test of nanogels.....	18
2.3.10.2 Cytocompatibility test of CUR-loaded nanogels.....	18
2.3.11 Cellular Uptake Study.....	19
CHAPTER III RESULTS AND DISCUSSION	20
3.1 Preparation of PPFPMA- <i>co</i> -POEGMA copolymer by conventional polymerization	20
3.1.1 Block copolymer.....	20

	Page
3.1.2 Random copolymer.....	24
3.2 Preparation of PFPMA-co-POEGMAM copolymer by post-polymerization modification	26
3.2.1 Synthesis of OEG-NH ₂	26
3.2.2 Post-polymerization modification of PFPMA with OEG-NH ₂	28
3.3 Micelles formation of amphiphilic copolymer.....	29
3.4 Formation of nanogels and subsequent post functionalization	32
3.5 Redox-responsiveness of nanogels.....	34
3.6 Preparation and characterization of hydrophobic drug-encapsulated nanogels	35
3.6.1 Encapsulation of NR.....	35
3.6.2 Encapsulation of CUR	37
3.7 Redox-responsive release of hydrophobic drug.....	38
3.7.1 NR release profile of NR-encapsulated nanogels.....	38
3.7.2 CUR release profile of CUR-encapsulated nanogels	40
3.8 Cytocompatibility of nanogels.....	40
3.8.1 Cytocompatibility against normal cells (L929).....	40
3.8.2 Cytocompatibility against cancer cells (MDA-MB-231).....	42
3.9 Cellular Uptake Study	43
CHAPTER IV CONCLUSION AND SUGGESTION.....	45
REFERENCES	47
APPENDIX.....	51
VITA.....	55

LIST OF FIGURES

Figures	Page
Figure 1.1 Chemical structures of activated ester monomers.	2
Figure 1.2 Schematic representation of design and synthesis of the polymeric nanogels [15].	3
Figure 1.3 Schematic representation of functionalization of different polymers using pfp and az activate ester groups [16].	4
Figure 1.4 Reaction scheme of polymeric precursor systems based on the reactive ester approach and their polymer-analogous conversion for radioactive labeling using [¹⁸ F]FETos [17].	5
Figure 1.5 Illustration of <i>in situ</i> forming reduction-sensitive nanogels for loading and triggered release of proteins [2].	6
Figure 1.6 Structure of 4-Cyanopentanoic acid dithiobenzoate (CPADB).	7
Figure 1.7 Mechanism of RAFT polymerization [18].	7
Figure 3.1 ¹ H NMR spectra (400 MHz, CDCl ₃) of (a) OEGMA monomer, (b) crude POEGMA, (c) POEGMA after dialysis and (d) POEGMA after precipitation.	21
Figure 3.2 ¹ H NMR spectra (400 MHz, CDCl ₃) of (a) PFPMA monomer, (b) PFPMA after purification, (c) crude PFPMA- <i>b</i> -POEGMA and (d) PFPMA- <i>b</i> -POEGMA after purification.	23
Figure 3.3 ¹ H NMR spectra (400 MHz, CDCl ₃) of (a) crude PFPMA- <i>r</i> -POEGMA, (b) PFPMA- <i>r</i> -POEGMA after purification.	25
Figure 3.4 Methodology for synthesis of OEG-NH ₂	26
Figure 3.5 (A) ¹ H NMR spectra in CDCl ₃ (a, b and c) and DMSO (d); (B) FTIR spectra.	27
Figure 3.6 FTIR (A) and ¹ H NMR spectra in CDCl ₃ (B) of (a) PFPMA, (b) OEG-NH ₂ , the copolymer with PFPMA: POEGMAM composition of (c) 73:27, (d) 46:54 and	

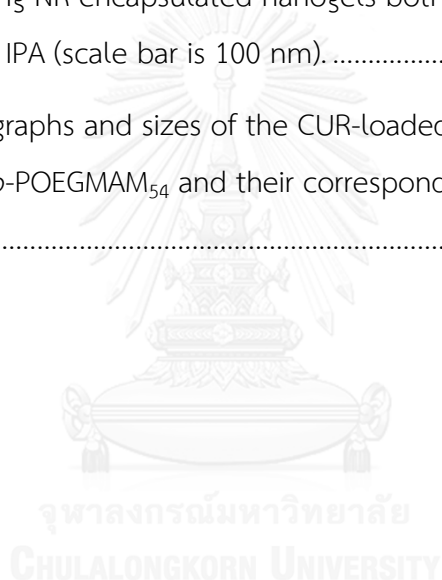
(e) 26:74. ^{19}F NMR spectrum of PPF $\text{PMA}_{73}\text{-CO-POEGMAM}_{27}$ is given in the inset of (B).	29
Figure 3.7 CMC determination of the copolymer using pyrene as fluorescence probe (A) P(PFP $\text{MA}_{73}\text{-CO-PEGMAM}_{27}$) and (B) P(PFP $\text{MA}_{46}\text{-CO-PEGMAM}_{54}$).	31
Figure 3.8 Reaction of post functionalization of copolymer	32
Figure 3.9 FTIR (A) and ^{19}F NMR spectra (400 MHz) (B) of PPF $\text{PMA}_{73}\text{-CO-POEGMAM}_{27}$ before (a) and after forming nanogels by crosslinking with 0.3 eq (b) and 0.6 eq (c) cystamine, and nanogels after crosslinking with 0.3 eq cystamine and post functionalization with IPA (d).	33
Figure 3.10 DLS profiles of nanogels prepared from PPF $\text{PMA}_{73}\text{-CO-POEGMAM}_{27}$ having 79 (A) and 43 %crosslinking before (B) and after (C) post functionalization with IPA in 20 mM GSH solution over time having PBS buffer pH 7.4 as a control.	35
Figure 3.11 Proposed CUR structure in (a) acidic, (b) neutral, and (c) basic environments [26].	38
Figure 3.12 NR release profiles from the NR-encapsulated nanogels after post functionalization with IPA without GSH at 25°C (blue triangles, solid line) and 37°C (red circles, solid line) and with GSH at 25°C (blue triangles, dashed line) and 37°C (red circles, dashed line) in aqueous solution of 20 mM GSH.....	39
Figure 3.13 CUR release profiles from the CUR-encapsulated nanogels without GSH (orange squares, dashed line) and with GSH (green diamonds, solid line) at 37°C in aqueous solution of 20 mM GSH.....	40
Figure 3.14 Percentage of cell viability of L929 cells after incubation for 24 h with micelles (a), nanogels before (b) and after (c) post functionalized with IPA as determined by MTT assay.	41
Figure 3.15 Percentage of cell viability of MDA-MB-231 cells after incubation for 24 h with nanogels (a), CUR-loaded nanogels (b) and CUR (c) as determined by MTS assay.....	42

- Figure 3.16** CLSM images of MDA-MB-231 cells incubated with free CUR and CUR-loaded nanogels having 10 mg/mL of CUR for 4 h. (blue fluorescence: nucleus staining dye, DAPI; green fluorescence: CUR; scale bar = 20 μm).....44
- Figure A1** ^1H NMR spectrum of PPF PMA_{73} -co-POEGMAM $_{27}$ in CDCl_352
- Figure A2** FTIR spectra of PPF PMA_{73} -co-POEGMAM $_{27}$ nanogels before and after induced hydrolysis in PBS at 37°C.....53
- Figure A3** ^{19}F NMR spectrum of PPF PMA_{73} -co-POEGMAM $_{27}$ nanogels indicating the release of pentafluorophenyl groups after induced hydrolysis in PBS at 37°C.....54



LIST OF TABLES

Table	Page
Table 3.1 TEM micrographs and sizes analyzed by TEM and DLS of the micelles assembled from the copolymers having different POEGMAM composition (scale bar is 100 nm).....	30
Table 3.2 TEM micrographs and sizes and zeta potential values determined by DLS of the NR-loaded micelles assembled from the PPFMA ₇₃ -co-POEGMAM ₂₇ and their corresponding NR-encapsulated nanogels both before and after post functionalization with IPA (scale bar is 100 nm).....	36
Table 3.3 TEM micrographs and sizes of the CUR-loaded micelles assembled from the PPFMA ₄₆ -co-POEGMAM ₅₄ and their corresponding CUR-encapsulated nanogels.	38



LIST OF SCHEMES

Scheme	Page
Scheme 1.1 Schematic illustration of preparation of drug-encapsulated nanogel for controlled release in the presence of glutathione (GSH).....	9



LIST OF ABBREVIATION

ACVA	: 4,4'-Azobis(4-cyanovaleric acid)
CLSM	: Confocal Laser Scanning Microscopy
CPADB	: 4-Cyano-4-(thiobenzoylthio)pentanoic acid
CUR	: Curcumin
DLS	: Dynamic Light Scattering
DCC	: dicyclohexylcarbodiimide
FTIR	: Fourier-Transform Infrared Spectroscopy
IPA	: <i>N</i> -isopropylamine
NR	: Nile red
OEGMAM	: oligoethylene glycol methacrylamide
OEG-NH ₂	: Oligo(ethylene glycol) methyl ether amine
PBS	: Phosphate buffered saline
PPFPMA	: Poly(pentafluorophenyl methacrylate)
RAFT	: Reversible addition-fragmentation chain transfer
TEM	: Transmission Electron Microscope

CHAPTER I

INTRODUCTION

1.1 Introduction

Polymeric nanoparticles which can encapsulate hydrophobic guest molecules within their interiors have been recognized as versatile cargos for many biomedical-related applications ranging from therapeutic vehicles for drug, gene, protein, and imaging agents to diagnostics [1-5]. Amphiphilic copolymers have continuously been demonstrated as promising materials for nanoparticle formation that can be conveniently driven by self-assembly process. Since this self-organized nanoassembly is emulsion-free process, possible contamination from emulsifier is no longer of concern. This issue is particularly critical if the generated nanocarriers are to be used in contact with biological systems.

Amphiphilic copolymers can be broadly categorized into two major types, block and random copolymers. Most attention has been paid to the self-assembly of block copolymers having well-defined structures with unique and excellent assembly characteristics [6-9] but the complicatedly synthetic methodologies can be time-consuming. In case of random copolymer, its synthesis is relatively easier than the block copolymer. Besides the conventional polymerization, the amphiphilic random copolymer can be prepared by another route that is post-polymerization modification.

Post-polymerization modification or polymer analogous reaction of activated ester-containing polymer [10] has recently emerged as an alternative and versatile route to generate amphiphilic copolymers. In other words, the functionalization to introduce either hydrophobic or hydrophilic entities would be performed on pre-synthesized polymers having active functional groups on their side chains. In principle, the ratio between hydrophobic and hydrophilic groups on the polymer backbone can be practically tuned by the extent of modification of which may be varied as a function

of reaction time and concentration of modifiers. Here in this research, pentafluorophenyl (PFP) ester-bearing polymer is chosen as a precursor polymer to be subjected to post-polymerization modification to generate amphiphilic random copolymers that are capable of forming self-assembled nanoparticles having potential for biomedical applications, particularly as carriers for bioactive compounds. It is more attractive than another previously invented precursor polymer based on *N*-acryloxysuccinimide (NAS) (**Figure 1.1**) derivative mainly due to its better solubility in many common organic solvents and higher hydrolytic stability of PFP in water and air than NAS [11, 12]. Additional advantage lies on the fact that the reaction of the pentafluorophenyl ester groups can be conveniently monitored by ^{19}F NMR spectroscopy [13]. PFP-bearing polymer also features a higher reactivity, allowing a practically quantitative conversion with nucleophilic modifiers, especially amines under mild conditions. The process has been reported as an effective route to amphiphilic random copolymers with controlled composition [14]. This activated ester-amine exchange yields a stable amide bond formation that is the basis of most biological systems. It is believed that this chemistry can potentially mimic the synthesis of many biological structures and help to comprehend their functions.

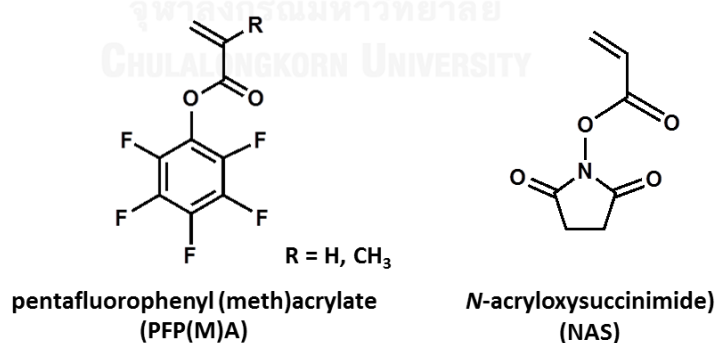


Figure 1.1 Chemical structures of activated ester monomers.

In 2012, Zhuang and coworkers [15] have prepared water-dispersible nanogels of amphiphilic random copolymers synthesized from pentafluorophenyl acrylate (PFPA) and poly(ethylene glycol) methacrylate (PEGMA) (**Figure 1.2**). The active PFPA groups of the copolymer were employed for crosslinking with designated diamines and

surface decoration with additional amine (i.e. *N*-isopropylamine (IPA), *N,N*-dimethylethylenediamine). Lipophilic guest molecules can be encapsulated during nanogel formation.

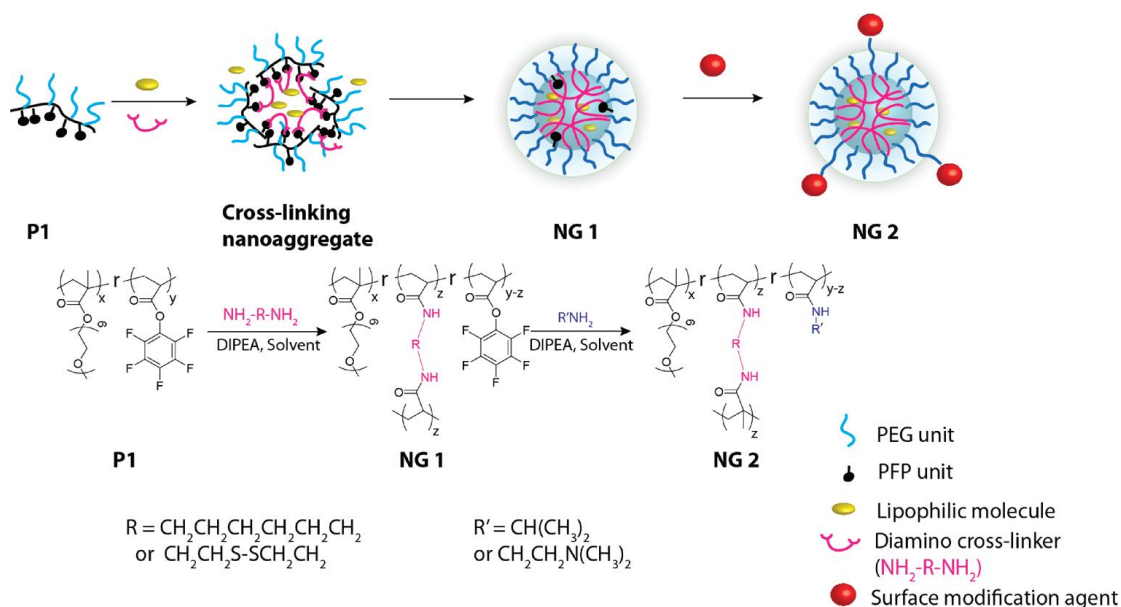


Figure 1.2 Schematic representation of design and synthesis of the polymeric nanogels [15].

In 2013, Li and coworkers [16] have synthesized both random and block copolymers of vinyl dimethyl azlactone (VDM) and pentafluorophenyl acrylate (PFPA). Functional units were introduced into polymer structures by successively reacting two different activated ester functionalities (pentafluorophenyl (PFP) ester and azlactone (AZ)) with various amine compounds (**Figure 1.3**). To exploit the difference in reactivity of the two activated esters (PFP and AZ) toward different amino compounds, they have demonstrated that a selective modification of the different activated ester groups can be done under a controlled manner, therefore capable of introducing various functional groups to the polymeric backbone. The developed functional copolymer obtained after polymer analogous reaction can self-assemble into nanoparticles.

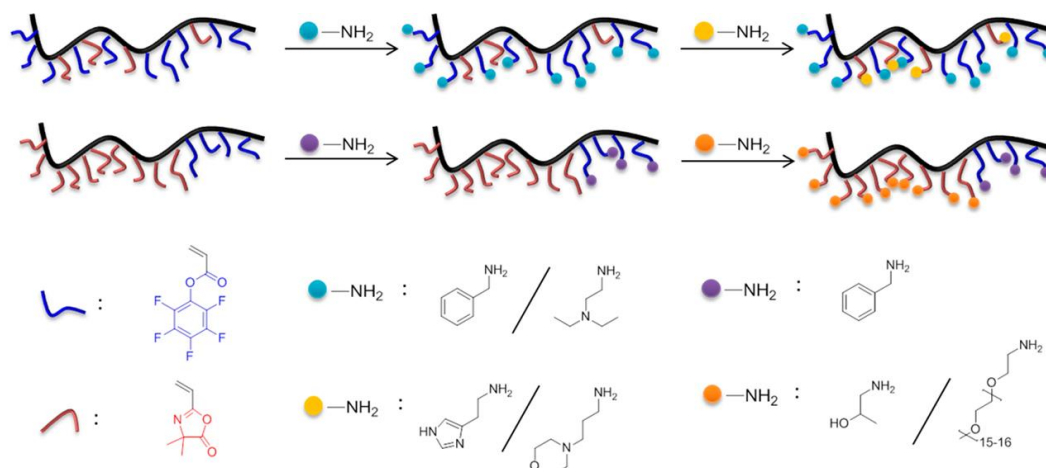


Figure 1.3 Schematic representation of functionalization of different polymers using pfp and az activate ester groups [16].

In 2011, Allmeroth and co-workers [17] have employed polymer analogous reaction to convert homopolymer of poly(pentafluorophenyl methacrylate) (PPFPMA) and copolymer between PFPMA and lauryl methacrylate (LMA) to *N*-(2-hydroxypropyl)methacrylamide homopolymer (PHPMA) and amphiphilic random copolymer between HPMA and LMA by reacting some of the PFP groups of the (co)polymer with 2-hydroxypropylamine. Small percentage of the remaining of PFP groups was conjugated with tyramine to form ^{18}F -labelable HPMA-based precursor (co)polymers. The radiolabeling procedure of the phenolic tyramine moieties via the secondary labeling synthon 2- ^{18}F fluoroethyl-1-tosylate (^{18}F FETos) (**Figure 1.4**) provided radiochemical fluoroalkylation so that pharmacokinetics and distribution of both the homopolymer and copolymer aggregates can be monitored by positron emission tomography (PET).

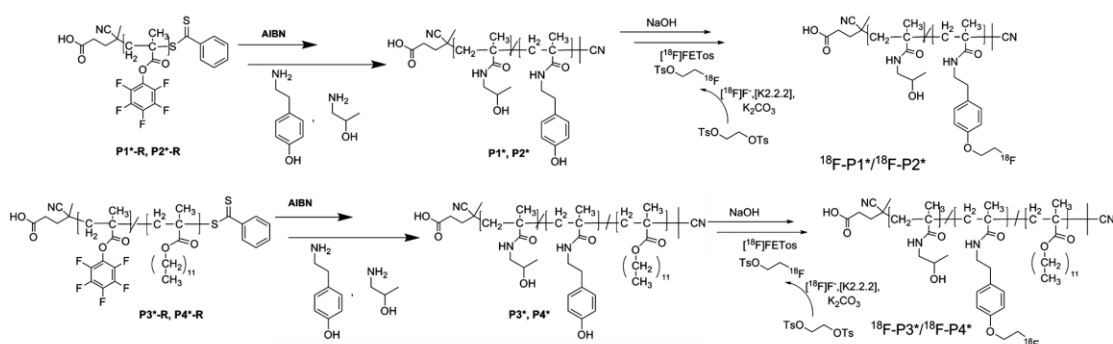


Figure 1.4 Reaction scheme of polymeric precursor systems based on the reactive ester approach and their polymer-analogous conversion for radioactive labeling using $[^{18}\text{F}]\text{FETos}$ [17].

In order to improve the nanoparticle stabilities under certain changes in biological systems, the hydrophobic core was stabilized by cross-linking. The thiol-responsive degradable cross-linker is promising to use for nanoparticle cross-linking. Due to reducing agents in the cytoplasm and nuclei of cells such as glutathione (GSH) having a pendant thiol ($-\text{SH}$) groups, the formed disulfide cross-links can be cleaved in response to reductive reactions, causing the nanoparticle dissociation, therefore the loaded molecules were allowed to release. Chen and co-workers [2] produced reduction-sensitive degradable nanogels developed based on poly(ethylene glycol)-*block*-poly(2-(hydroxyethyl) methacrylate-*co*-acryloyl carbonate) (PEG-*P*(HEMA-*co*-AC)) block copolymers for encapsulation and triggered intracellular release of proteins (**Figure 1.5**). Cystamine was used as crosslinker of the nanogels via nucleophilic ring-opening of cyclic carbonate with amino groups of cystamine. The obtained nanogels show excellent stability with limited protein release under physiological conditions. They were also rapidly de-crosslinked and disassociated under intracellular-mimicking reductive environments, resulting in efficient intracellular protein release.

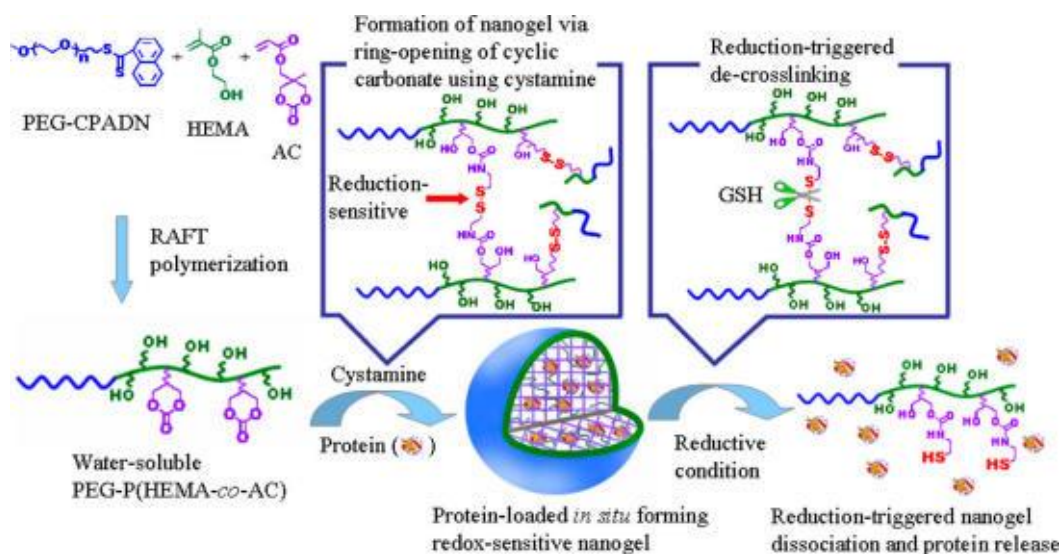


Figure 1.5 Illustration of *in situ* forming reduction-sensitive nanogels for loading and triggered release of proteins [2].

There is a variety of methodology for polymer synthesis. Recently, reversible addition-fragmentation chain transfer (RAFT) polymerization, one kind of controlled radical polymerization, is a living polymerization involving a conventional radical polymerization in the presence of a reversible chain transfer reagent (CTA) such as 4-cyanopentanoic acid dithiobenzoate (CPADB, **Figure 1.6**). By controlling the concentration of CTA, it is possible to generate polymer with controlled molecular weight and low polydispersity index (PDI) [18]. In addition, the RAFT is attractive for synthesizing a variety of polymers. Some monomers capable of polymerizing by RAFT include acrylates, acrylamides as well as other vinyl monomers.

There are four steps in RAFT polymerization with thiocarbonylthio CTA involving initiation, chain transfer, reinitiation and equilibration as illustrated in **Figure 1.7**.

1. Initiation: The reaction is started by radical initiators such as 4,4'-Azobis(4-cyanovaleric acid) (ACVA) and 2,2'-Azobis(2-methylpropionitrile) (AIBN). In this step, the initiator (I) can react with a monomer to generate radical species starting active polymerizing chain.

2. Reversible chain transfer: The active chain (P_n) can react with the dithioester that eliminate the leaving group (R). This is a reversible step having an intermediate species capable of loss either the active species (P_n) or the leaving group (R).

3. Reinitiation: The leaving group which is radical specie then reacts with other monomers to start another active polymer chain. This active chain (P_m) is then able to go through the reversible chain transfer or chain equilibration steps.

4. Equilibration: This is the fundamental step in the RAFT which can control the majority of the active propagating species to be the dormant thiocarbonyl compound. This helps to limit the possibility of chain termination. Active polymer chains (P_m and P_n) are in an equilibrium whereas one polymer chain is in the dormant stage (bound to the thiocarbonyl group), the other is still active in polymerization process.

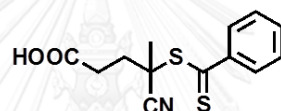


Figure 1.6 Structure of 4-Cyanopentanoic acid dithiobenzoate (CPADB).

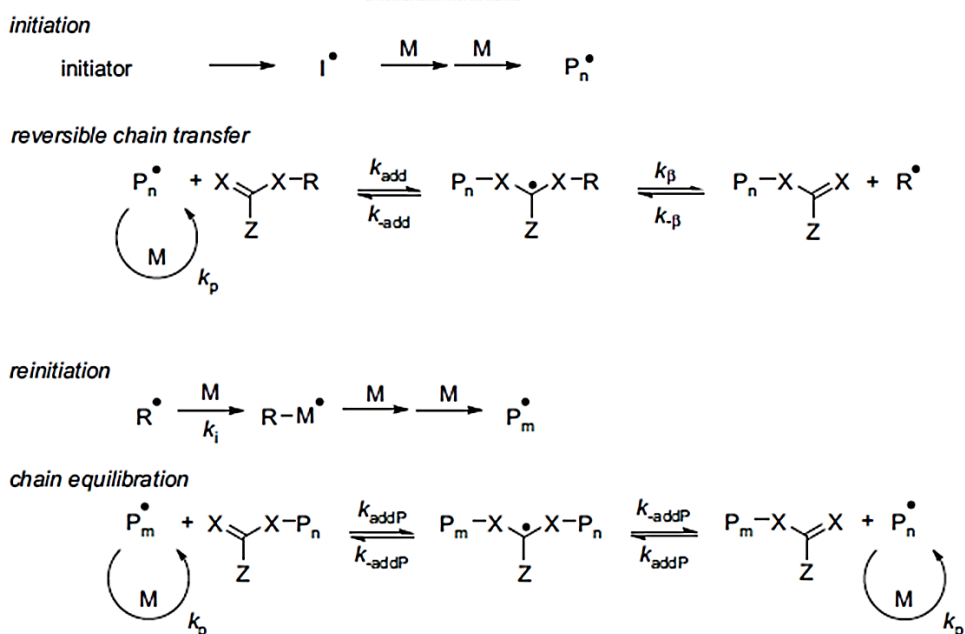


Figure 1.7 Mechanism of RAFT polymerization [18].

Unlike the works mentioned above, here preparation of amphiphilic copolymers by both conventional polymerization and post-polymerization modification routes were the scope of this thesis. In case of the conventional polymerization, both block and random amphiphilic copolymer are attempted to synthesize with PFPMA and OEGMA monomers by RAFT. In addition, the random copolymer can be created via post-polymerization modification of PFPMA with nucleophilic modifier having hydrophilic entity, amine-terminated oligoethylene glycol (OEG-NH₂). The inherit hydrophobicity of the remaining PFP groups available in the amphiphilic copolymer allows for hydrophobic guest molecules encapsulation and nanoparticle formation to simultaneously occur upon water-induced micellization. It should also be emphasized that micelles can be formed without the requirement for additional post-functionalization with another hydrophobic modifier. The second post-functionalization by crosslinker dually functionalized with amine, cystamine is performed thereafter to retain structural integrity of the nanoparticles by forming nanogels. By employing this disulfide crosslinker, a release of encapsulated hydrophobic molecule, Nile red (NR) and curcumin (CUR) can be induced by redox-trigger such as glutathione (GSH), a naturally available reducing agent inside the cells. Last step of modification with isopropylamine is carried out in order to get rid of the remaining PFP groups in the nanogels to prevent the release of pentafluorophenyl groups upon hydrolysis that may potentially cause adverse effect on biological systems under physiological condition. Overall concept of this research work is summarized in **Scheme 1.1**.

3. Preparation of drug-loaded redox-responsive nanogels and modification of the nanogels via post-polymerization modification.

4. Release study of the drug-loaded nanogels under condition with and without GSH as reducing agent.

5. *In vitro* cytotoxicity test of the developed nanogels against normal cells and cancer cells.

6. Cellular uptake study of the developed nanogels using confocal laser scanning microscopy.



CHAPTER II

MATERIALS AND METHODS

2.1 Materials

All solvents used for reactions are analytical grade and used as received, unless otherwise specified. 1,4-Dioxane (anhydrous, 99.9%) and pentafluorophenol (PFP) were commercially available from Merck, Germany. Dichloromethane (DCM) was dried over CaH_2 under reflux and N_2 atmosphere. Aqueous solutions were made with Milli-Q water purified by Millipore Milli-Q system that involves reverse osmosis, ion exchange, and filtration steps. 4,4'-Azobis(4-cyanovaleric acid) (ACVA), dicyclohexylcarbodiimide (DCC), anhydrous *N,N*-dimethylformamide (DMF, 98.8%), methacrylic acid (MA), *N*-isopropylamine (IPA), Nile red (NR), oligo(ethylene glycol) methacrylate (average M_n 360), phosphate buffered saline, pH 7.4 (PBS), pyrene, *p*-toluenesulfonyl chloride and triethylamine were purchased from Sigma-Aldrich, USA and used as received. 4-Cyanopentanoic acid dithiobenzoate (CPADB) was obtained from Santa Cruz biotechnology, USA. Sodium azide was obtained from Riedel de Haën. Oligo(ethylene glycol) 350 monomethyl ether and triphenylphosphine were purchased from Fluka. 3-(4,5-Dimethylthiazol-2-yl)-5-(3-carboxymethoxyphenyl)-2-(4-sulfophenyl)-2H-tetrazolium (MTS) assay reagent containing the electron coupling agent phenazine ethosulfate (PES) was purchased from Promega (USA). Curcumin (Acros Organics) was used directly after purchase.

2.2 Instrumentations

The polymers before and after modification were characterized by nuclear magnetic resonance spectroscopy (NMR) using a Varian, model Mercury-400 nuclear magnetic resonance spectrometer (USA) operating at 400 MHz and Fourier transform infrared spectroscopy (FTIR) using a Nicolet Impact 6700 FT-IR. ^{19}F NMR spectra were recorded on a Bruker AVANCE III HD (500 MHz) FT-NMR spectrometer. UV-Vis spectra

were recorded on an Agilent 8453 UV-Vis spectroscopy in a quartz cell with 1 cm path length. Molecular weight of the polymers were measured by Waters 600 controller chromatograph equipped with two HR (Waters) columns (HR2 and HR4) (MW resolving range = 100-500,000 Da) at internal column temperature of 35°C and a refractive index detector (Waters 2414). THF was used as a solvent for the polymers and as an eluent for GPC analysis with a flow rate of 1.0 mL/min. Five polystyrene standards (996–188,000 Da) were used for generating a calibration curve. The hydrodynamic size of micelles were determined using a dynamic light scattering (DLS) instrument (Zetasizer Nano ZS, Malvern Instrument Ltd., U.K. equipped with a He-Ne laser beam at 658 nm) at a fixed scattering angle of 173°. The sample refractive index (RI) was set at 1.59 for polystyrene. All samples were filtered through a Millipore 0.45 µm Nylon membrane before analysis. The morphology of nanoparticles was analyzed by transmission electron microscopy (TEM) by a JEOL JEM-2100 (Japan). MTT assay and MTS assay were performed by Thermo Scientific Multiscan FC microplate reader at 540 nm and Biochrom® Anthos 2010 (UK) microplate reader at 492 nm. The confocal laser scanning microscopy (CLSM) of cell analysis was performed using FluoView FV10i confocal microscope (OLYMPUS).

2.3 Experimental Procedure

2.3.1 Synthesis of pentafluorophenyl methacrylate

Pentafluorophenyl methacrylate (PFPMA) was synthesized according to a modified method from previously published works [19, 20]. PFP was dissolved in dry DCM. MA was slowly added to the solution mixture on ice bath, and DCC in dry DCM was then added dropwise to the mixture. After stirring for 2 h, the precipitate of dicyclohexylurea was filtered, washed thoroughly with DCM. The filtrate was evaporated, and the crude product was then purified by flash column chromatography (column material: silica gel; solvent: hexane). Pure colorless liquid was obtained in 67% yield.

^1H NMR (400 MHz, CDCl_3): δ /ppm: 6.45 (t, 1H), 5.91 (t, 1H), 2.07 (t, 3H); ^{19}F NMR (CDCl_3): δ /ppm: 162.57 (dd, 2F), 158.22 (t, 1F), 152.80 (d, 2F); FT-IR (ATR-mode): 1780 cm^{-1} (C=O reactive ester band), 1529 cm^{-1} (C=C aromatic band)

2.3.2 Synthesis of homopolymer by RAFT polymerization

2.3.2.1 Synthesis of poly(pentafluorophenyl methacrylate) (PPFPMA)

Poly(pentafluorophenyl methacrylate) (PPFPMA) was synthesized following the previously reported method [14]. PFPMA (2.5 M), CPADB (25 mM), and ACVA (5 mM) were dissolved in dry 1,4-dioxane (5 mL) in a vial. The mixed solution in the sealed vial was purged with N_2 gas for 30 min and then immersed in a preheated oil bath at 70°C for 12 h. The solution was cooled down to room temperature before precipitated in methanol three times, and dried under vacuum. The product was obtained as pink powder with 71% yield.

2.3.2.2 Synthesis of poly(oligo(ethylene glycol) methacrylate) (POEGMA)

OEGMA monomer (1M), CPADB (50 mM), and ACVA (6.2 mM) were dissolved in dry 1,4-dioxane (3 mL). The vial was sealed with a rubber septum and the solution was deoxygenated by purging with nitrogen gas for 30 min. The mixture was then carried out at 70°C for 2 h. The polymer solution was purified by precipitation with diethylether five times or dialysis against DMF for three days and ethanol for two days. The product was then dried under vacuum to obtain red viscous fluid.

2.3.3 Preparation of poly(oligo(ethylene glycol) methacrylate)-co-poly(pentafluorophenyl methacrylate) (POEGMA-co-PPFPMA) copolymer

2.3.3.1 Synthesis of random copolymer of poly(oligo(ethylene glycol) methacrylate)-*ran*-poly(pentafluorophenyl methacrylate) (POEGMA-*r*-PPFPMA)

The comonomer composition of PFPMA:OEGMA in the ratio of 1:1 was synthesized by RAFT polymerization. PFPMA (0.5 M), OEGMA (0.5 M), CPADB (40

mM), and ACVA (5 mM) were dissolved in dry 1,4-dioxane (1.5 mL). The mixture was sealed and was bubbled with nitrogen gas for 30 min. The vial was put in an oil bath at 70°C for 2 h. The resulting polymer was purified by precipitation with diethylether five times. The product was then dried under vacuum to obtain viscous fluid.

2.3.3.2 Synthesis of block copolymer of poly(pentafluorophenyl methacrylate)-*block*-poly(oligo(ethylene glycol) methacrylate) (PPFPMA-*b*-POEGMA)

According to the previously mentioned method (2.3.2.1), PPFPMA was first synthesized and used as a macro chain transfer agent for POEGMAM synthesis. The purified PPFPMA (10 mM), OEGMA (1 M), and ACVA (1.25 mM) were added to a vial followed by 2 mL of dry 1,4-dioxane. The vial was sealed with a rubber septum and the solution was purged with nitrogen gas for 30 min. Polymerization was conducted at 70°C for 2 h. The polymer solution was precipitated in diethylether five times and finally dried under vacuum at room temperature.

2.3.4 Synthesis of oligo(ethylene glycol) methyl ether amine (OEG-NH₂)

Oligo(ethylene glycol) monomethyl ether (OEG-OH) (7.720 mL, 24.00 mmol, 1 eq.) and triethylamine (4.992 mL, 36.00 mmol, 1.5 eq.) were dissolved in dry DCM (25 mL) and the mixture was then cooled to 0 °C. A solution of *p*-toluenesulfonyl chloride (4.580 g, 24.00 mmol, 1 eq.) in DCM (25 mL) was then slowly added dropwise. The solution was stirred for 2 hours at 0 °C and overnight at room temperature. The reaction was quenched by addition of 1.2 M HCl solution and the layers were then separated. The aqueous layer was extracted twice with DCM and (20mL). The combined organic layers were washed with brine (3x15mL) and were passed through anhydrous Na₂SO₄, filtered and evaporated to dryness. The crude product was purified by flash column chromatography (column material: silica gel; solvent: ethyl acetate:methanol 99:1) to obtain 10.3811 g (20.591 mmol, 86%) of oligo(ethylene glycol) methyl ether tosylate (OEG-OTs) as colorless oil.

The tosylate product (9.7336 g, 19.310 mmol, 1 eq.) was dissolved in *N,N*-dimethylformamide (DMF) (40 mL) and sodium azide (3.1380 g, 48.280 mmol, 2.5 eq.) was added. The flask was purged with nitrogen for 30 min and the mixture was stirred in a preheated oil bath at 67 °C for 12 h. The resulting mixture was diluted with water (40 mL) and further stirred 30 min. The solution was cooled to 0 °C and was then extracted with diethylether (5x30 mL). After combination of the organic layers, the diethylether layer was washed with brine once, passed over Na₂SO₄ and finally concentrated to afford the azide product (5.2637g, 13.460 mmol, 70%).

Oligo(ethylene glycol) methyl ether azide (OEG-N₃) (5.2359 g, 13.390 mmol, 1 eq.) was dissolved in diethyl ether (40 mL) and the solution was cooled to 0 °C. Triphenyl phosphine (5.0650 g, 19.310 mmol, 1.4 eq.) was added and the solution was stirred at 0 °C for 1 h and 1.5 h at room temperature. The mixture reaction was quenched with DI water (40 mL) and was then vigorously stirred for 4 h. Toluene (30 mL) was added and the mixture was stirred overnight. After decantation, the aqueous layer was extracted with toluene (15 mL). The aqueous layer was lyophilized to yield oligo(ethylene glycol) methyl ether amine (OEG-NH₂) (2.7913 g, 7.6474 mmol, 57%) was obtained as yellow oil.

¹H NMR (400 MHz, DMSO-d₆): δ /ppm 3.4-3.7 (m, 28 H), 3.3 (s, 3 H); FT-IR (ATR-mode): 2870 cm⁻¹ (C-H stretching), 1596 cm⁻¹ (N-H bending), 1100 cm⁻¹ (C-O stretching)

2.3.5 Post-polymerization modification of PFPMA with OEG-NH₂

PPFPMA (1 eq. of PFP groups) was dissolved in dry DMF. OEG-NH₂ of varied equivalent to PFP groups of PFPMA (0.25, 0.50, or 0.75 eq.) in DMF was mixed with PFPMA. The reaction mixture was stirred at ambient temperature for 24 h. The polymer solution was precipitated in hexane. Amphiphilic copolymer of poly(pentafluorophenyl methacrylate)-*co*-poly(oligo(ethylene glycol) methacrylamide) (PPFPMA-*co*-POEGMAM)) having varied composition was obtained

after re-dissolving the precipitate in THF and re-precipitating in hexane for two more times.

2.3.6 Critical micelle concentration (CMC)

CMC of the copolymers were determined using pyrene as a fluorescence probe according to the previously published method [21]. The polymeric solutions were varied in different concentrations in a range of 0.3-12 mg/ml. To all of the solutions, Five μL pyrene solution in acetone (1.2×10^{-4} M) was added and then the mixture were dissolved in 1 mL PBS. The emission spectra were recorded on a UV-vis spectrophotometer.

2.3.7 Preparation of hydrophobic molecule-loaded nanogels

2.3.7.1 Preparation of NR-loaded nanogels

The copolymer, PFPMA₇₃-co-POEGMAM₂₇ having designated composition (21.0 mg, 0.056 mol PFPMA, 1 eq.) and NR (10.5 mg) were dissolved together in 100 μL THF. PBS buffer (3 mL) was added dropwise under vigorous stirring. Cystamine of varied equivalent to PFP groups of the copolymer (0.3 or 0.6 eq.) used as a crosslinker was added to stabilize the assembled nanoparticles by forming nanogels. The reaction was performed for 24 h at ambient temperature. The NR-loaded nanogels were purified by dialysis against Milli-Q water for 3 days with water changes twice per day (dialysis membrane, MWCO = 3,500 Da) to remove unreacted crosslinker. The dispersion was filtered through a 0.45 μm syringe filter to remove the excess insoluble NR.

2.3.7.2 Preparation of CUR-loaded nanogels

The PFPMA₄₆-co-POEGMAM₅₄ copolymer (21.0 mg, 0.035 mol PFPMA, 1 eq.) and CUR (10.5 mg) were dissolved in THF (100 μL). Three mL of PBS buffer was added slowly under vigorous stirring. Cystamine (0.6 eq.) used as a crosslinker was added to stabilize the assembled nanoparticles by forming nanogels. The reaction was performed for 24 h at ambient temperature. The CUR-loaded

nanogels were purified by dialysis against Milli-Q water for 3 days with water changes twice per day (dialysis membrane, MWCO = 3,500 Da) to remove unreacted crosslinker. The dispersion was filtered through a 0.45 μm syringe filter to remove the excess insoluble CUR.

2.3.8 Post functionalization of NR-loaded nanogels

N-Isopropylamine (IPA) as another nucleophilic modifier was excessively (71.8 μL , 0.836 mmol) added into the NR loaded nanogels suspension (7 mg/mL, 3 mL) for 24 h at ambient temperature in order to eliminate the remaining PFP moieties left in the nanogels. The nanogels were purified by dialysis against Milli-Q water with water changes twice per day for 3 days (dialysis membrane, MWCO = 3,500 Da) to remove unreacted IPA.

2.3.9 Redox-responsive release studies

2.3.9.1 Redox-responsive release of NR

The suspension of NR-encapsulated nanogels (7 mg/mL, 2 mL) was adjusted to pH 7.4 by adding PBS buffer. GSH was added to the suspension of NR-encapsulated nanogels to give GSH concentration in the suspension of 20 mM. The absorbance spectra of NR encapsulated in nanogels were monitored by UV/vis spectroscopy at certain time points and percentages of NR release were calculated by $(A_0 - A_t)/A_0 \times 100\%$, where A_0 and A_t represent the absorbance ($\lambda = 543 \text{ nm}$) at $t = 0$ and a specific incubation time point, respectively. The release studies were performed at 25 and 37°C.

2.3.9.2 Redox-responsive release of CUR

The suspension of CUR-encapsulated nanogels (7 mg/mL, 2 mL) was adjusted to pH 7.4 by adding PBS buffer. GSH was added to the suspension of NR-encapsulated nanogels to give GSH concentration in the suspension of 20 mM. The absorbance spectra of CUR encapsulated in nanogels were monitored by UV/vis spectroscopy at certain time points and percentages of CUR release

were calculated by $(A_0 - A_t)/A_0 \times 100\%$, where A_0 and A_t represent the absorbance ($\lambda = 425 \text{ nm}$) at $t = 0$ and a specific incubation time point, respectively. The release studies were performed at 37°C .

2.3.10 Cytocompatibility tests

2.3.10.1 Cytocompatibility test of nanogels

Mouse fibroblast L929 cells were cultured in RPMI 1640 medium supplemented with 5% fetal bovine serum (FBS), penicillin (100,000 U/L) and streptomycin (100 mg/mL). The cells were then plated at approximately 2×10^4 cells/well into a tissue culture 96-well plates in 200 μL medium per well. Various concentrations of the suspension of copolymeric micelles both before and after forming nanogels were incubated with the cells at 37°C under 5% CO_2 containing atmosphere for 24 h. 3-(4,5-Dimethylthiazol-2-yl)-2,5-diphenyltetrazolium bromide (MTT) solutions (10 μL) was then added into each well. After 4 h of incubation, the supernatant solution was replaced with DMSO (150 μL) in order to dissolve the purple crystals of formazan. The optical density of the samples was measured by a microplate reader at 540 nm.

2.3.10.2 Cytocompatibility test of CUR-loaded nanogels

Cytocompatibility of CUR-loaded nanogels were analyzed using a MTS cell viability assay. Suspension of mammary gland adenocarcinoma (MDA-MB-231) cells (5,000 cells/mL, 100 μL) was seeded into a tissue culture 96-well plates, cultured for 24 h. The media was replaced with 100 μL of various concentrations of CUR-loaded nanogels, nanogels and CUR in Minimum Essential Medium with Earle's Balanced Salts (MEM/EBSS, GE Healthcare HyClone) and maintained at 37°C under 5% CO_2 condition for 24 h. 100 μL of the same concentrations of CUR-loaded nanogels, nanogels and CUR in MEM were defined as blank. MTS solution (10 μL) was added. After incubation for 4 h, the cell suspension was measured by a microplate reader at 492 nm.

2.3.11 Cellular Uptake Study

MDA-MB-231 cells (2.5×10^5 cells) were plated into an 8-well Lab-Tek II Chamber Slide w/Cover RS Glass Slide in 500 μL of MEM, and cultured for 24 h. The medium was removed and a total of 500 μL of free CUR, CUR-loaded nanogels suspension was added immediately. After 4h incubation, the cells were softly washed with PBS buffer twice. Nucleus staining dye, DAPI (0.02 mg/mL, 100 μL) was added, followed by incubation in dark with shaking for 5 min. After staining step, these cells were softly washed with PBS buffer three times. Chamber was removed from glass slide. The glass slide was dried and was then dropped with anti-fade reagent (MOWIOL). It was finally closed with cover slip. The cell analysis was performed by confocal microscope using FV10-ASW 4.2 Viewer as software.



CHAPTER III

RESULTS AND DISCUSSION

3.1 Preparation of PPFMA-co-POEGMA copolymer by conventional polymerization

3.1.1 Block copolymer

POEGMA-*b*-PPFMA block copolymer, with OEGMA and PPFMA monomers in the ratio of 1:1, was prepared, starting with POEGMA as the first block. OEGMA was initially polymerized by RAFT with CPADB:ACVA in ratio of 4:1. Unfortunately, the polymer had become gel since 2 h and the resulting product cannot dissolve in any solvent. Therefore we changed the condition of polymerization to use CPADB:ACVA in ratio 8:1 in order to reduce the polymerization rate and let the chain transfer agent (CPADB) control the MW more effectively using reaction time of 4 h. The obtained product was very viscous which was purified by dialysis against DMF for three days and ethanol for two days before drying under vacuum. However, the product was not pure because it still contained OEGMA monomer as displayed in ^1H NMR at δ 1.9, 5.6 and 6.1 ppm for allylic and olefinic protons, respectively (**Figure 3.1c**). After that, the purification step was improved from dialysis to reprecipitation. The polymer was dissolved in THF and precipitated again in diethylether. Although this reprecipitation was repeated more than four times, the product still contained OEGMA monomers (**Figure 3.1d**). Due to the high viscosity of POEGMA, the polymer may trap the monomer. For all the reasons mentioned above, this POEGMA is quite difficult to purify to be pure that residue monomer can affect the polymerization in the next step. So we tried to synthesize the block copolymer by another route starting the first block with PPFMA.

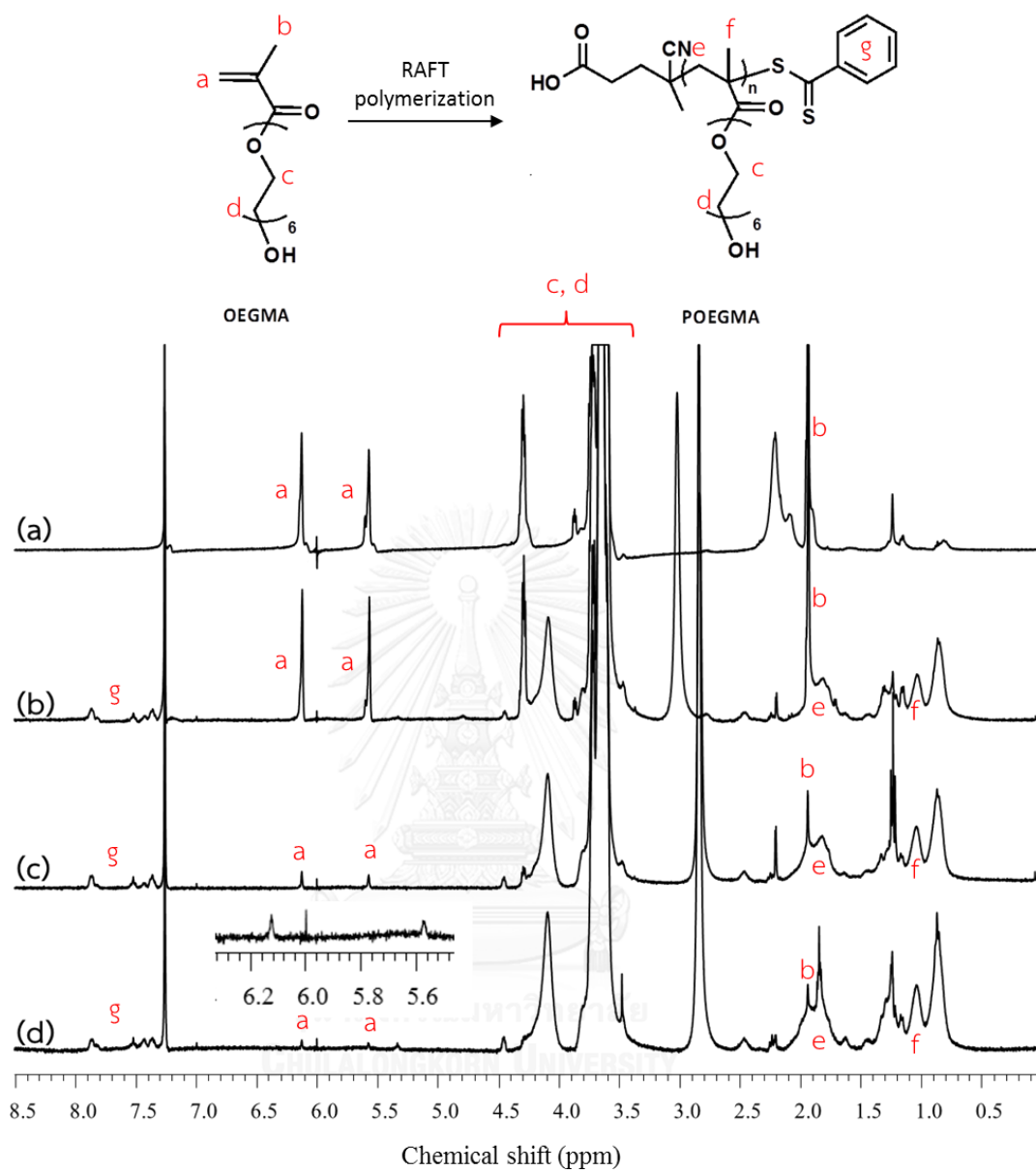
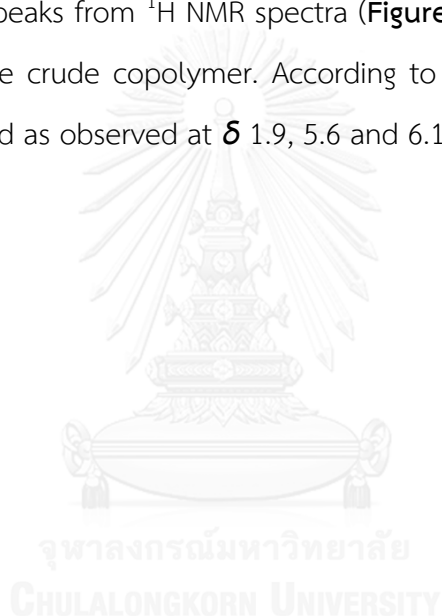


Figure 3.1 ^1H NMR spectra (400 MHz, CDCl_3) of (a) OEGMA monomer, (b) crude POEGMA, (c) POEGMA after dialysis and (d) POEGMA after precipitation.

Alternatively, PPFMA was first polymerized (**Figure 3.2b**) by RAFT with CPADB:ACVA in ratio of 4:1 and using PPFMA monomer, which was synthesized via esterification reaction of pentafluorophenol and methacrylic acid. The PPFMA was used as a macro-CTA for the POEGMA synthesis. The PPFMA macro-CTAs with molecular weights of 15.4 kDa with PDI 1.37 (theoretical $M_n = 13.0$ kDa for target degree of polymerization of 50) were prepared as evaluated by GPC. POEGMA was very viscous as mentioned before so this property negatively affected the purification process of the copolymer. The product was not pure even though the observed OEGMA peaks from ^1H NMR spectra (**Figure 3.2d**) significantly decreased comparing with the crude copolymer. According to ^1H NMR spectra, the OEGMA monomer remained as observed at δ 1.9, 5.6 and 6.1 ppm.



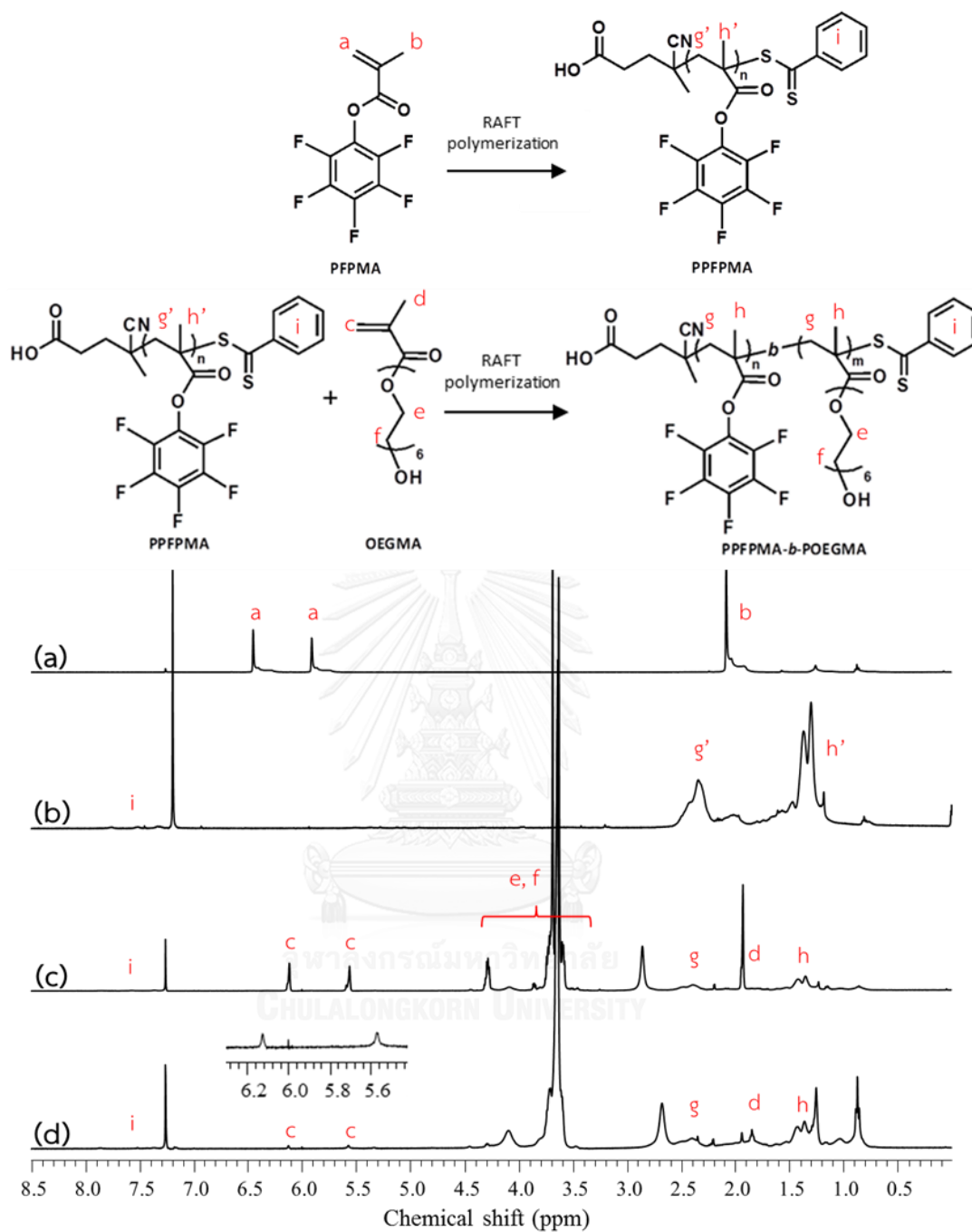


Figure 3.2 ^1H NMR spectra (400 MHz, CDCl_3) of (a) PFPMA monomer, (b) PPFMA after purification, (c) crude PPFMA-b-POEGMA and (d) PPFMA-b-POEGMA after purification.

3.1.2 Random copolymer

PPFPMA-*r*-POEGMA random copolymer was prepared using two monomers; PFPMA and OEGMA with the ratio of 1:1. The obtained copolymer was purified by reprecipitation five times but the product was still impure (**Figure 3.3b**) as observed in the case of POEGMA block copolymer. Both OEGMA and PFPMA monomer peaks also appeared in the ^1H NMR spectra at δ 1.9, 5.6 and 6.1 for OEGMA, and 5.9 and 6.5 for PFPMA, respectively.

All of three methods used for preparation of POEGMA-containing copolymer failed due to the purification step. The remaining OEGMA monomers cannot be removed completely from the highly viscous polymer products. The procedure for preparation of the desired amphiphilic copolymer was therefore modified from conventional polymerization to post-polymerization modification.



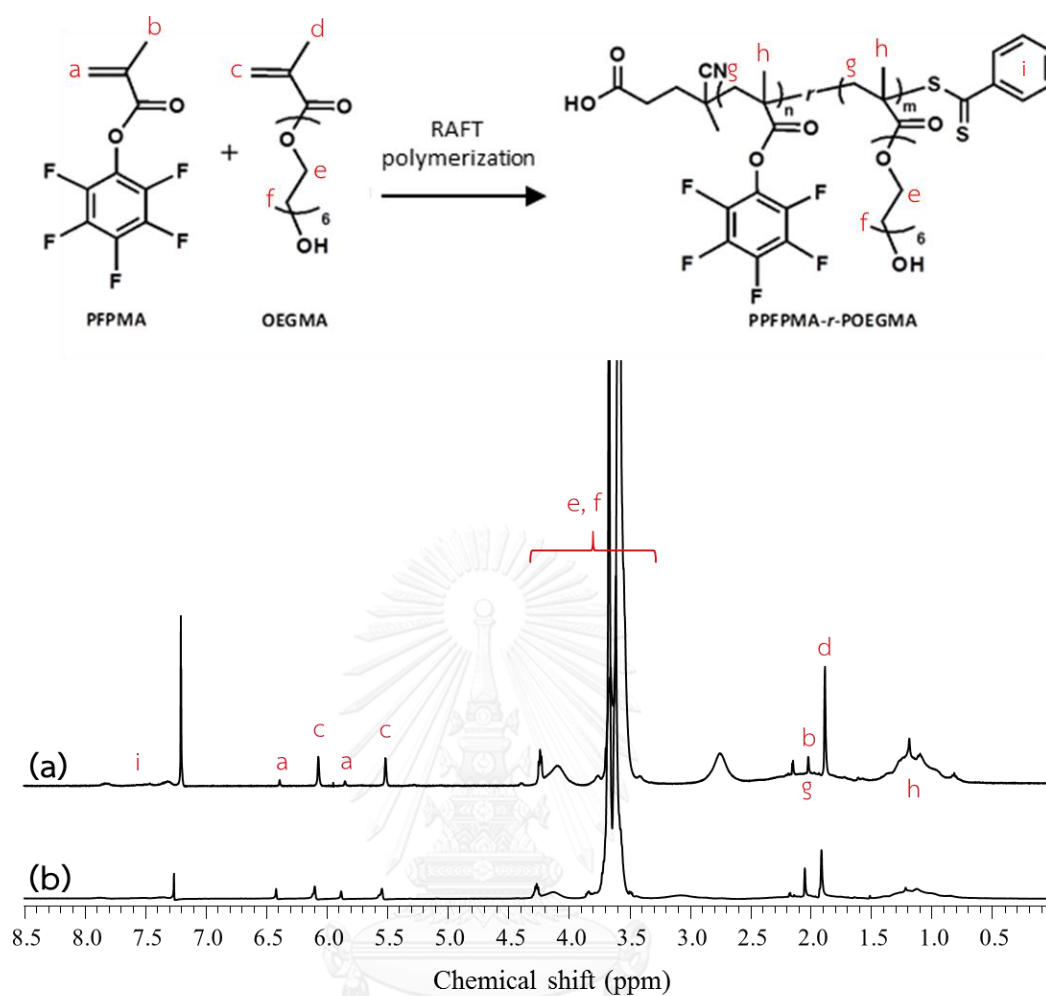


Figure 3.3 ^1H NMR spectra (400 MHz, CDCl_3) of (a) crude PPFMA-*r*-POEGMA, (b) PPFMA-*r*-POEGMA after purification.

3.2 Preparation of PFPMA-co-POEGMAM copolymer by post-polymerization modification

3.2.1 Synthesis of OEG-NH₂

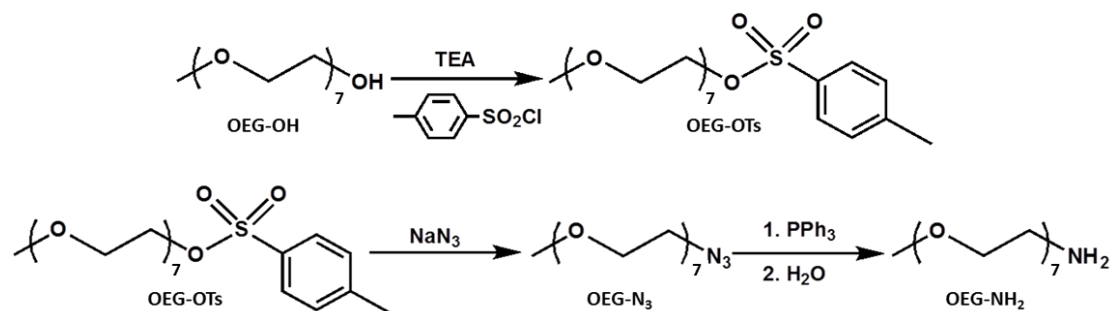


Figure 3.4 Methodology for synthesis of OEG-NH₂

The desired oligo(ethylene glycol) methyl ether amine (OEG-NH₂) was synthesized from the OEG-OH by three steps including tosylation, nucleophilic substitution with sodium azide (NaN₃), followed by Staudinger reduction (**Figure 3.4**).

According to the tosylation step, the terminal hydroxyl group of OEG-OH was converted to tosylates by treating with *p*-toluenesulfonyl chloride. The reaction was purified by column chromatography in order to remove unreacted *p*-toluenesulfonyl chloride, yielding the tosylate product 86% yield. ¹H NMR spectra (**Figure 3.5A**) show the characteristic signals of OEG-OTs at 7.9, 7.4, and 3.4-3.7 ppm which are attributed to aromatic protons of tosylate and -CH₂O- and CH₃O- of OEG moiety.

The second step was substitution of OEG-OTs with azide to obtain OEG-N₃ with 70% yield. The disappearance of aromatic protons signal (δ 7.4 and 7.9 ppm) in ¹H NMR spectrum (**Figure 3.5A**, spectrum b) after azide substitution indicated that the tosyl group was successfully eliminated yielding OEG-N₃. The successful reaction was also confirmed by the appearance peak of azide signal at 2100 cm⁻¹ from FTIR technique (**Figure 3.5B**).

The azide group at the chain end of OEG was converted to an amine group by Staudinger reduction using triphenylphosphine. After the reduction, OEG-NH₂ was obtained as yellow oil with 57% yield. The product was confirmed by FTIR showing the disappearance of azide peak (2100 cm⁻¹) and the appearance of amine peak (1596 cm⁻¹) (Figure 3.5B, spectrum d).

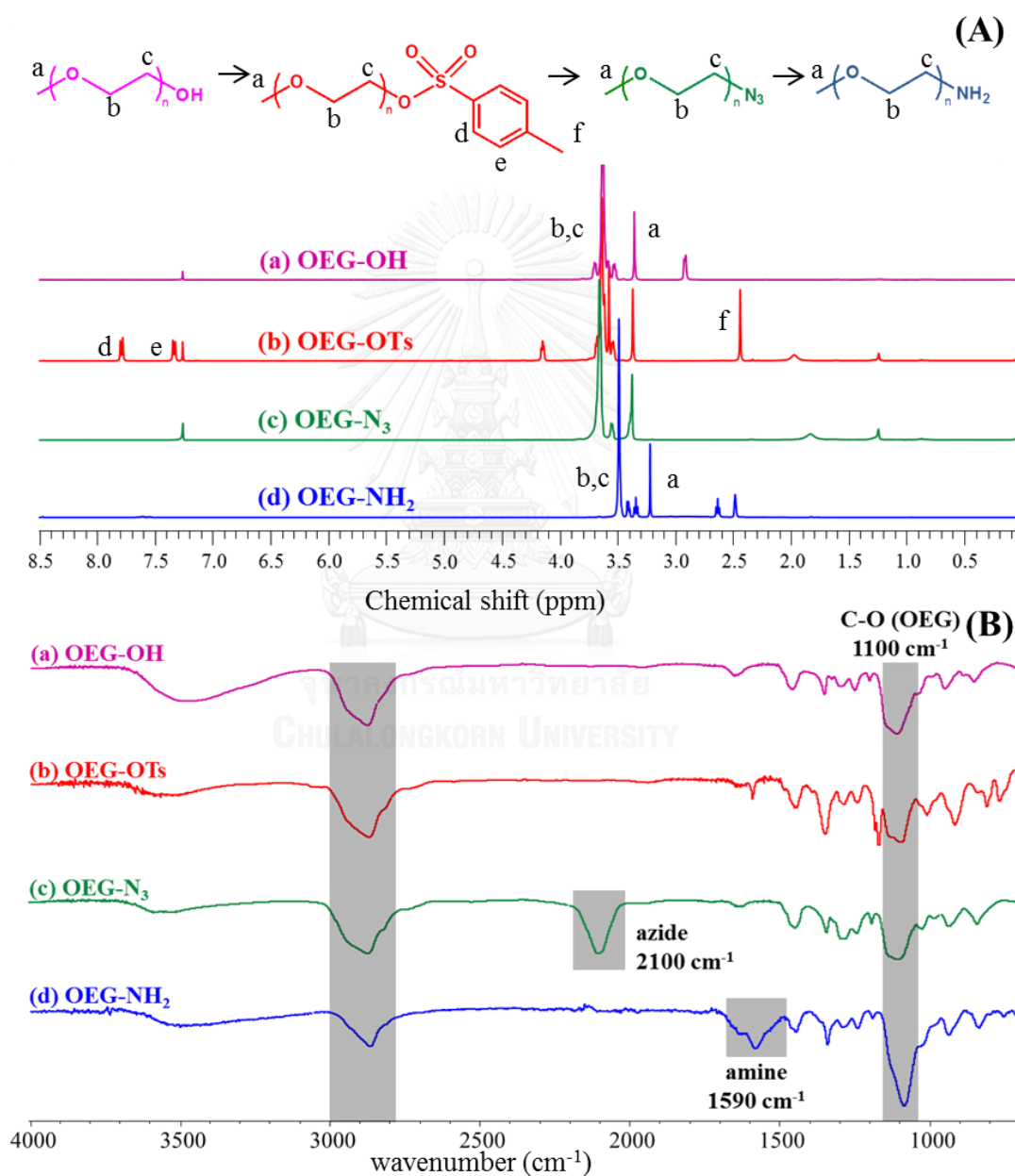


Figure 3.5 (A) ¹H NMR spectra in CDCl₃ (a, b and c) and DMSO (d); (B) FTIR spectra.

3.2.2 Post-polymerization modification of PFPMA with OEG-NH₂

By performing RAFT polymerization, PFPMA with M_n of 25.6 kDa and PDI of 1.34 was obtained as evaluated by GPC. The fact that the M_n of the polymer closely resembles the theoretical value of 25,493 Da for target degree of polymerization of 100 with relatively narrow PDI suggests that the polymerization was reasonably under control. Post-polymerization modification of PFPMA with OEG-NH₂ yielded amphiphilic OEG-containing copolymer (PFPMA-co-POEGMAM). The emergence of amide (C=O stretching) signal at 1666 cm⁻¹ and the disappearance of amine (N-H bending) signal of OEG-NH₂ at 1596 cm⁻¹ in FTIR spectra of the copolymers (**Figure 3.6A**) suggested that there was amide bond formation as a result of modification. The remaining PFP groups in the copolymer can be evidenced from the ester C=O signal at 1780 cm⁻¹. This signal is proportionally decreased as the POEGMA composition increased which can be varied as a function mole equivalent of OEG-NH₂ employed for post-polymerization modification. In addition, the small peak at 1721 cm⁻¹ which can be assigned to C=O stretching of COOH strongly signified that slight hydrolysis of PFPMA unavoidably occurred due to small amount of water as azeotropic mixture of OEG-NH₂. The extent of hydrolysis estimated by FTIR was in a range of 4-12%. Copolymer composition should be more accurately determined by ¹H NMR analysis (See calculation in appendix). ¹H NMR spectra depicted in **Figure 3.6B** revealed the characteristic signals of PFPMA-co-POEGMAM at 3.4-3.7, 3.3, 2.3, and 1.3 ppm which are attributed to -CH₂O- and CH₃O- of OEG moiety, as well as -CH₂- and -CH₃ of the copolymer backbone, respectively. The composition of POEGMAM in the copolymer was found to be 27, 54, and 74% upon the post functionalization of PFPMA with 0.25, 0.50, and 0.75 eq. of OEG-NH₂, respectively. The presence of remaining PFP groups in the copolymer was also evidenced by ¹⁹F NMR analysis. There are peaks appearing at -151.7, -152.7 (ortho), -158.2 (para), and -163.3 (meta) ppm in the ¹⁹F NMR spectrum of PFPMA₇₃-co-POEGMAM₂₇ shown in the inset of **Figure 3.6B**.

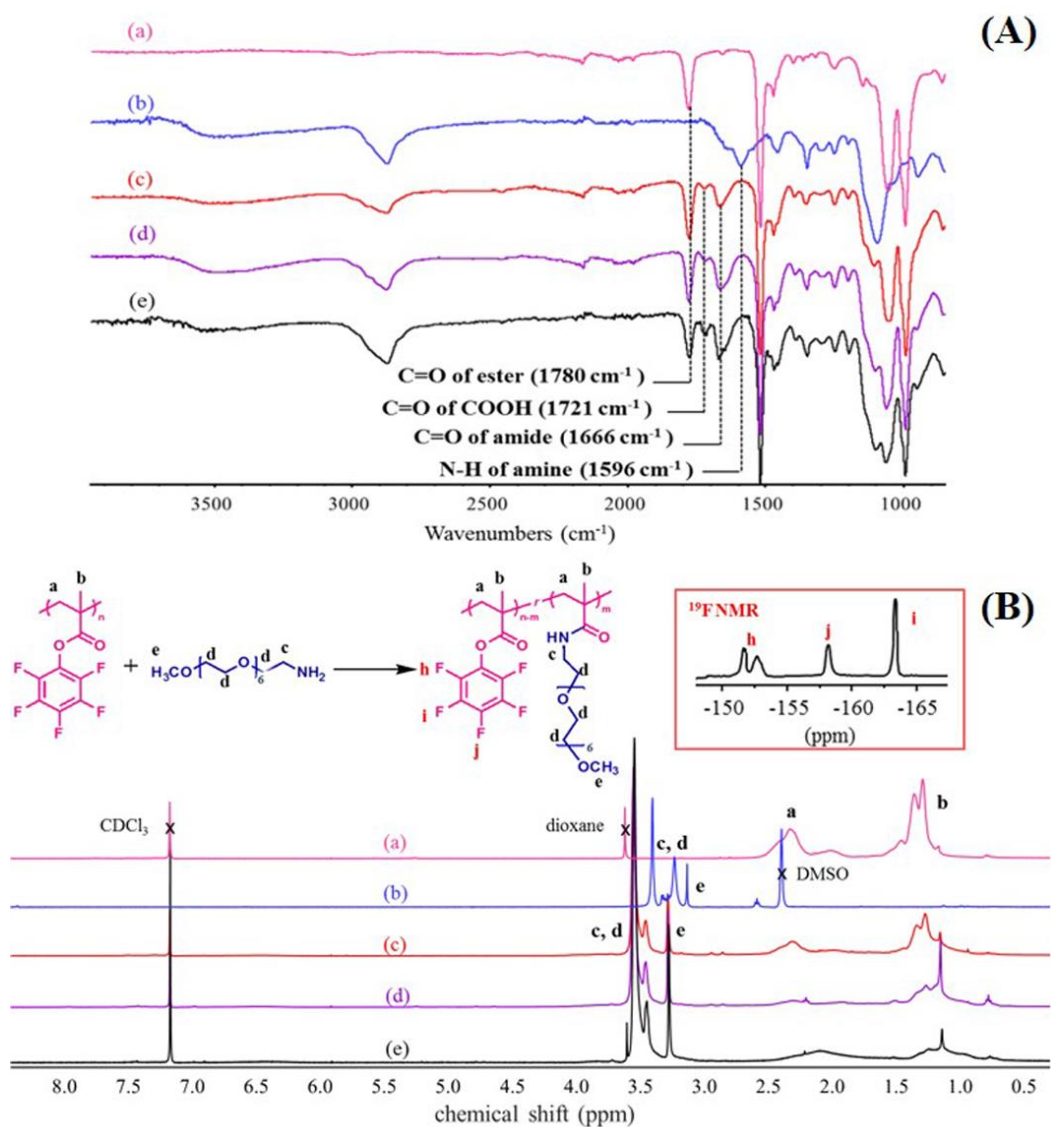


Figure 3.6 FTIR (A) and ^1H NMR spectra in CDCl_3 (B) of (a) PPFPPMA, (b) OEG-NH₂, the copolymer with PPFPPMA: POEGMAM composition of (c) 73:27, (d) 46:54 and (e) 26:74. ^{19}F NMR spectrum of PPFPPMA₇₃-co-POEGMAM₂₇ is given in the inset of (B).

3.3 Micelles formation of amphiphilic copolymer

The amphiphilic copolymers with three different compositions of POEGMAM (27, 54 and 74%) could self-assemble in aqueous media to yield well-defined spherical-like micelles of which morphologies and size are shown in **Table 3.1**. The sizes of the micelles characterized by both techniques are well below 100 nm with reasonably narrow particle size distribution. These dimensions are well suitable for

intracellular drug carriers of which diameters should approximately be 200 nm or less [1]. The micelles tended to progressively increase in size as the composition of hydrophilic POEGMAM shell increased. The fact that the diameters detected by the solution-based technique, DLS are greater than those evaluated by TEM truly emphasized the swellability of the micelles in water.

Table 3.1 TEM micrographs and sizes analyzed by TEM and DLS of the micelles assembled from the copolymers having different POEGMAM composition (scale bar is 100 nm).

	PPFPMA ₇₃ -co-POEGMAM ₂₇	PPFPMA ₄₆ -co-POEGMAM ₅₄	PPFPMA ₂₆ -co-POEGMAM ₇₄
TEM (nm)	28 ± 9	38 ± 11	41 ± 8
DLS (nm)	46 ± 0.1 PDI = 0.199	61 ± 0.2 PDI = 0.237	67 ± 2 PDI = 0.540

The critical micelle concentration (CMC) of the copolymers was determined using a pyrene fluorescence probe. The plot of fluorescence intensities against the log of the polymer concentration were recorded (**Figure 3.7**). The onset of the change in slope of the line was taken as the CMC. **Figure 3.7A** and **Figure 3.7B** show that the CMC values of the copolymer PPFPMMA₇₃-co-POEGMAM₂₇ and PPFPMMA₄₆-co-POEGMAM₅₄ were about 7 and 4 mg/mL, respectively. The CMC decreased with increasing hydrophilic composition part, OEGMAM, in this case. This is because hydrophilicity can enhance the thermo-dynamical stability and can thus promote self-assembly process [22]. The CMC of PPFPMMA-co-POEGMAM obtained are relatively high as compared with those of OEG-based block copolymers of which hydrophobic and hydrophilic entitles are well-ordered. This may presumably due to random distribution of hydrophobic

and hydrophilic entities along the polymer chains that weaken the driving force of self-assembly. It is also possible that the hydrophobic PFPMA units are amorphous so that greater concentration of polymer is thus required to form micelles. This has been previously described by others for OEG-based copolymer, that the micelle formed with amorphous cores exhibited higher CMC than those with semicrystalline cores [23].

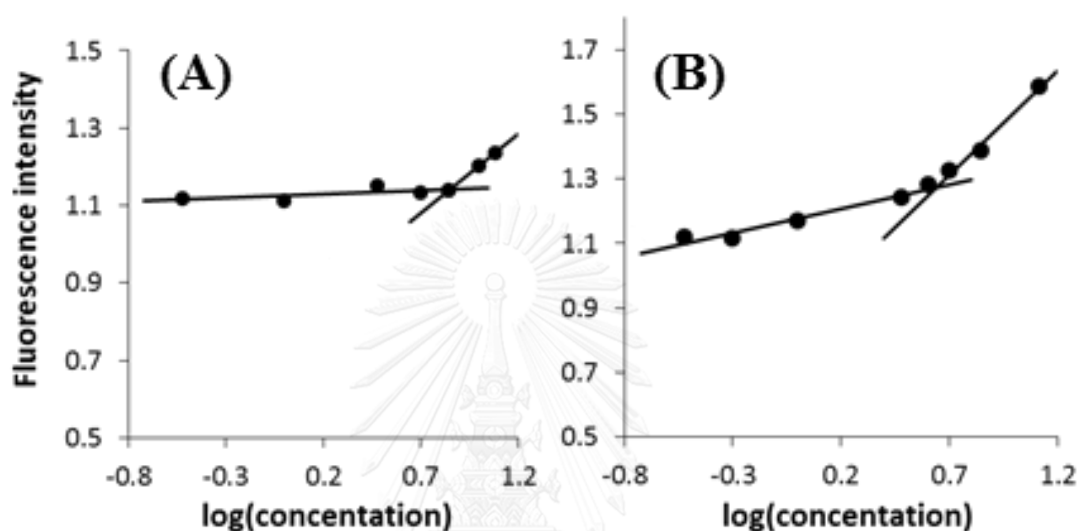


Figure 3.7 CMC determination of the copolymer using pyrene as fluorescence probe (A) P(PFPMA₇₃-co-PEGMAM₂₇) and (B) P(PFPMA₄₆-co-PEGMAM₅₄).

3.4 Formation of nanogels and subsequent post functionalization

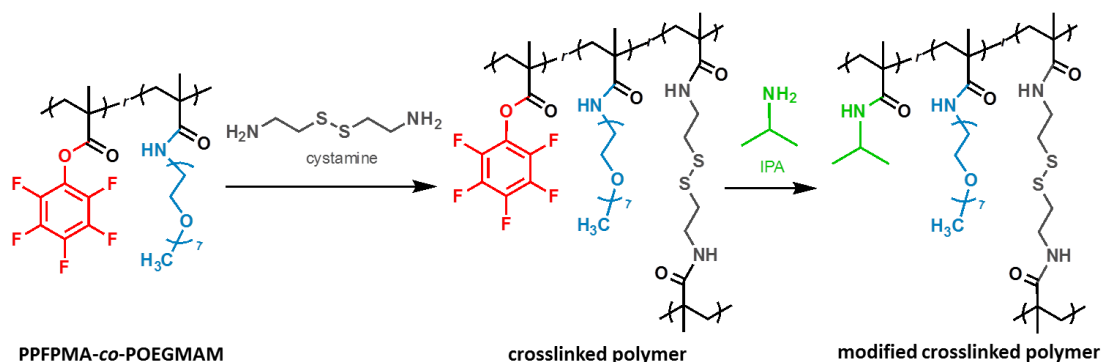


Figure 3.8 Reaction of post functionalization of copolymer

The copolymer having 27% POEGMAM (PPFPMA₇₃-co-POEGMAM₂₇) was selected for the following investigation mainly because of their smallest dimension and highest PFPMA composition which should allow for a convenient handling of multi-step post-polymerization modification to follow thereafter. Nanogels can be formed upon micellar crosslinking of the assembled amphiphilic copolymer with cystamine (**Figure 3.8**). This diamine modifier provides dithiol linkage to stabilize the micelles and simultaneously inherits redox-responsiveness to the resulting nanoassemblies. The extent of crosslinking was also varied as a function of cystamine equivalent added in comparison with PFP groups in the copolymer. As shown in **Figure 3.9A**, the FTIR pattern of the nanogels obtained after crosslinking with 0.3 eq cystamine was not much changed from that of the assembled micelles before crosslinking. Three characteristic C=O signals still remain except the ratio between the signal at 1666 cm⁻¹ to that at 1780 cm⁻¹ which corresponded to the amide C=O and ester C=O stretching, respectively, became slightly higher implying that some of the PFP groups (43% as estimated by FTIR) were consumed upon crosslinking. Level of crosslinking can also be elevated by increasing the quantity of cystamine to 0.6 eq. The relative ratio between the signals at 1666 cm⁻¹ to that at 1780 cm⁻¹ was much higher suggesting that the majority of PFP groups (79% as estimated by FTIR) were employed. Further post functionalization of the nanogels having 43% crosslinking was done thereafter using

IPA as non-toxic nucleophilic modifier. Apparently, only trace signal due to ester C=O stretching peak was detected indicating that PFP groups were almost entirely removed. There was approximately 2% PFP groups left in the nanogels according to FTIR analysis. This assumption was also verified by ^{19}F NMR analysis (Figure 3.9B). Only trace amount of characteristic signals of PFP groups (-151.7, -152.7 (ortho), -158.2 (para), and -163.3 (meta) ppm) was observed.

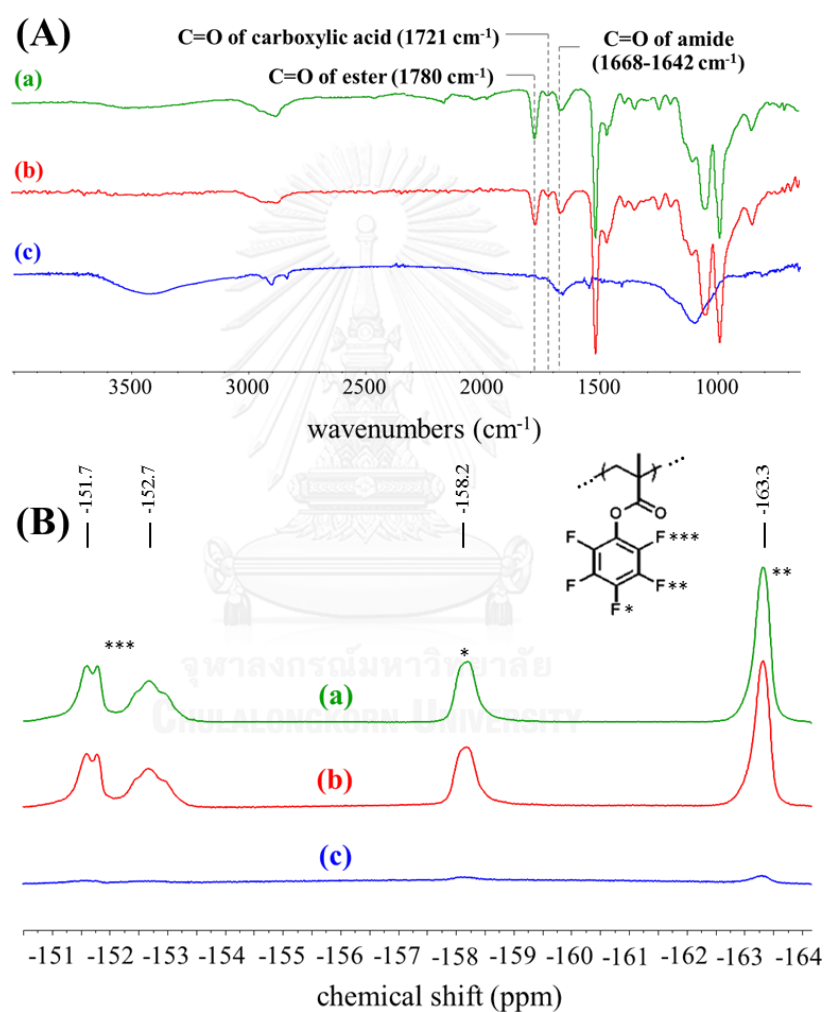


Figure 3.9 FTIR (A) and ^{19}F NMR spectra (400 MHz) (B) of PFPMA₇₃-co-POEGMAM₂₇ before (a) and after forming nanogels by crosslinking with 0.3 eq (b) and 0.6 eq (c) cystamine, and nanogels after crosslinking with 0.3 eq cystamine and post functionalization with IPA (d).

3.5 Redox-responsiveness of nanogels

Glutathione (GSH), a tripeptide found in most living cell, contains sulfhydryl groups of cysteine which can cleave disulfide linkage [24]. Therefore, GSH was selected as a representative cellular reducing agent [25-27]. DLS was used as a tool to determine redox-responsive property of the nanogels by monitoring the change in their size under reducing environment in the presence of GSH as a function of time. As shown in **Figure 3.10**, the size of nanogels having 79% crosslinking remained mostly unchanged in the presence of GSH for up to 20 h. There was a small peak appearing above 1,000 nm implying possible aggregation of the nanogels. However, degradation was found to be more obvious for the nanogels having 43% cross-linking. Before incubation with GSH (at 0 h), the average diameter of nanogels both before and after post functionalization with IPA in PBS buffer (pH 7.4) were 50 nm (PDI = 0.239) and 53 nm (PDI = 0.214), respectively. In the presence of 20 mM GSH, the peaks around 50 nm still remained but the particle size distribution became broad and multimodal ranging from approximately 250 nm to the aggregated form with the diameter over 2,000 nm within 2 h. This strongly suggested that GSH can destroy the disulfide bridges within the nanogels, resulting in particle dissociation, agglomeration and change in particle size. At 20 h, the broader distributions and the decrease of intensity of original peak (at 50 and 53 nm) were observed in both nanogels. In contrast, in the absence of GSH, the size distribution of the two nanogels maintained their stability for up to 20 h. This set of data also suggested that the stability and redox responsive property of the nanogels was not affected by post functionalization by IPA.

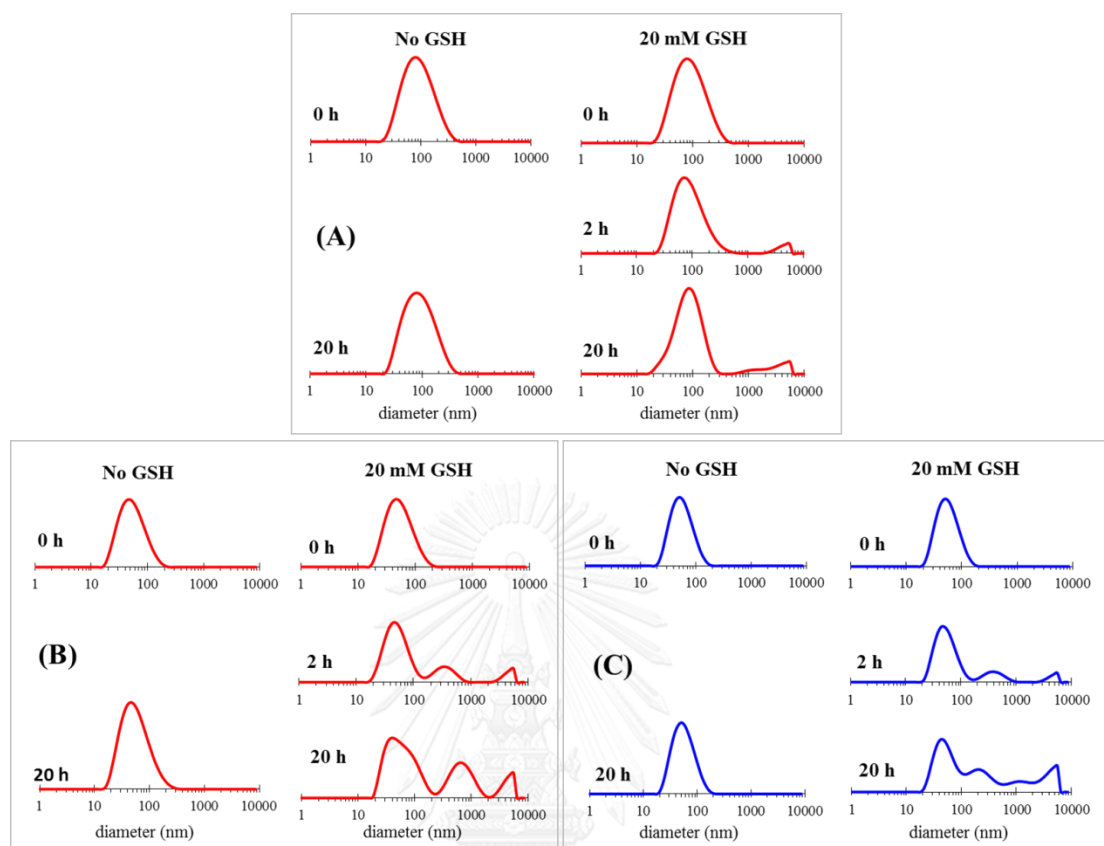


Figure 3.10 DLS profiles of nanogels prepared from PFPMA₇₃-co-POEGMAM₂₇ having 79 (A) and 43 %crosslinking before (B) and after (C) post functionalization with IPA in 20 mM GSH solution over time having PBS buffer pH 7.4 as a control.

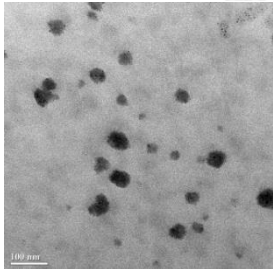
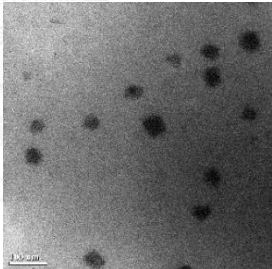
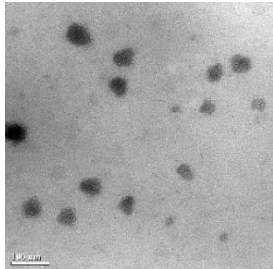
3.6 Preparation and characterization of hydrophobic drug-encapsulated nanogels

3.6.1 Encapsulation of NR

To investigate the capability of the nanoparticles to store hydrophobic molecules by hydrophobic interactions, encapsulation of a hydrophobic guest molecule model, NR, was first studied. As an inherently water-insoluble dye, NR was dissolved in THF with the PFPMA₇₃-co-POEGMAM₂₇ copolymers before micellar assembly in water. The crosslinker, cystamine was added thereafter to provide stability to the micelles and form NR-encapsulated nanogels. The presence of NR inside the nanoparticles was confirmed by pink suspension being observed which can be detected by UV-vis spectroscopy (absorbance peak at 543 nm). As

determined by TEM, the nanogels are spherical in shape with quite narrow size distribution after NR encapsulation (**Table 3.2**). The NR-encapsulated nanogels were slightly smaller in size than the original non-crosslinked micelles without encapsulated NR. Post functionalization with IPA to remove the hydrophobic PFP groups caused the nanogels to be more hydrophilic so that they were more swellable and became larger in size. The zeta potential of all particles are slightly negative indicating the particle shell layer is dominated by OEG entities independent of NR encapsulation, crosslinking, and post functionalization.

Table 3.2 TEM micrographs and sizes and zeta potential values determined by DLS of the NR-loaded micelles assembled from the PFPMA₇₃-co-POEGMAM₂₇ and their corresponding NR-encapsulated nanogels both before and after post functionalization with IPA (scale bar is 100 nm).

	NR-encapsulated micelles	NR-encapsulated nanogels	NR-encapsulated nanogels after post functionalized with IPA
			
TEM (nm)	45 ± 7	41 ± 7	44 ± 8
DLS (nm)	55 ± 2 PDI = 0.221	44 ± 1 PDI = 0.343	63 ± 1 PDI = 0.429
ζ - potential (mV)	-11.0 ± 1.1	-9.5 ± 0.3	-10.4 ± 0.9

3.6.2 Encapsulation of CUR

Anticancer drug, curcumin (CUR), was chosen to be encapsulated in the nanoparticles because it strongly exhibits therapeutic activity against various cancers [28]. In order to encapsulate CUR in nanogels, the desired copolymer used for forming the particles was changed from PPFMA₇₃-co-POEGMAM₂₇ to PPFMA₄₆-co-POEGMAM₅₄. To load CUR or other hydrophobic drugs containing hydroxyl group, the drug-loaded nanogel or micelle cannot be modified with basic amino modifiers, such as IPA. It is because the hydroxyl group of these hydrophobic drugs can be easily deprotonated by basic amine as shown in **Figure 3.11**. That allowed the drug become more hydrophilic so it can conveniently leak out from hydrophobic core to surrounding water, resulting in indirectly affecting the drug loading content. Although the reaction was performed in PBS buffer (pH 7.4), amine, which is strong base, was needed to excessively add in order to eliminate toxic PFP moieties. Therefore the resulting pH became as high as 12-13. However, crosslinking process was still carried out all residue PFP groups inside particle to remove the toxic moiety of PFP without further amine functionalization. Preparing the CUR-loaded nanogel, PPFMA₄₆-co-POEGMAM₅₄ and CUR were dissolved in THF and were then prepared to be CUR-loaded micelle in water. Crosslinker, cystamine, was added to stabilize the nanoparticle and the CUR-loaded nanogel was obtained. The presence of CUR inside the nanoparticles was confirmed by yellow suspension being observed which can be measured by UV-vis spectroscopy (absorbance peak at 425 nm). According to TEM images, the nanogels are spherical in shape with quite narrow size distribution (**Table 3.3**).

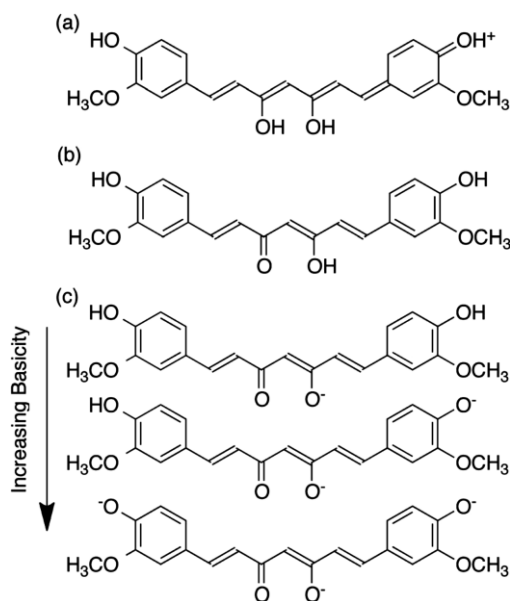


Figure 3.11 Proposed CUR structure in (a) acidic, (b) neutral, and (c) basic environments [26].

Table 3.3 TEM micrographs and sizes of the CUR-loaded micelles assembled from the PPFMA₄₆-co-POEGMAM₅₄ and their corresponding CUR-encapsulated nanogels.

	CUR-encapsulated micelles	CUR-encapsulated nanogels
TEM (nm)	75 ± 14	61 ± 14

3.7 Redox-responsive release of hydrophobic drug

3.7.1 NR release profile of NR-encapsulated nanogels

The NR release of the NR-encapsulated nanogels prepared by PPFMA₇₃-co-POEGMAM₂₇ was measured by the change of UV absorbance ($\lambda = 543$ nm) as demonstrated in **Figure 3.12**. In the absence of GSH, there was no NR release at

25°C indicating that NR is stably trapped inside the nanogels. This characteristic is highly favorable from application perspective in which the drug loaded nanogels can be stored for a longer time before usage. Raising the temperature to 37°C, approximately 10% cumulative NR release was detected. It was suspected that there might be a small extent of disulfide bond breaking at such an elevated temperature so that some NR can be released out. Redox-responsive release can be realized in the presence of GSH. NR as high as 70% was released after 95 h at 25°C while the percentage of NR release reached 94% over the same period of time at 37°C. The superior release behavior at elevated temperature was ascribed also as a consequence of temperature-promoted degradation of disulfide crosslinking so that more NR can be released.

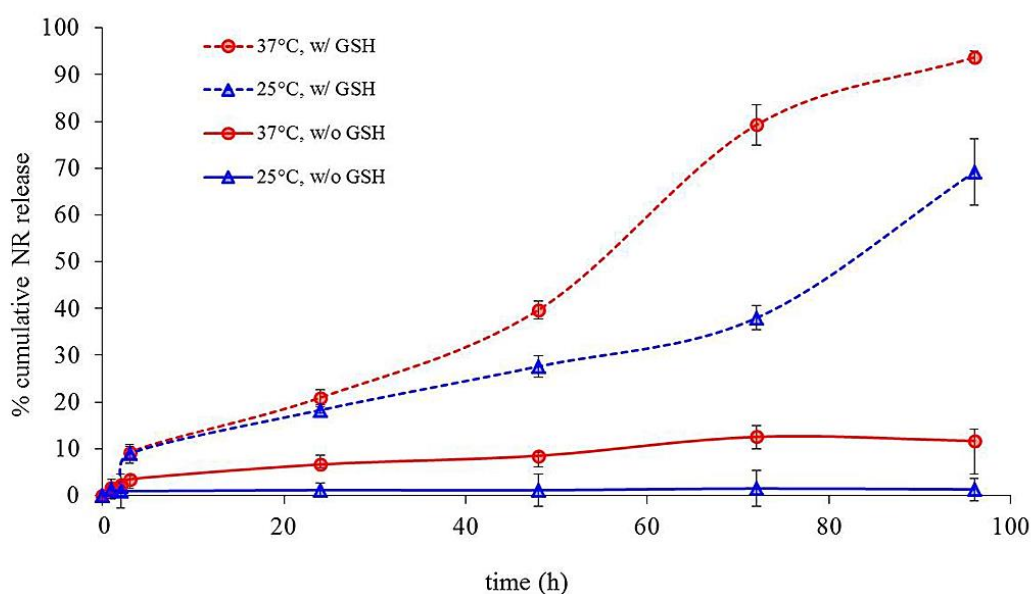


Figure 3.12 NR release profiles from the NR-encapsulated nanogels after post functionalization with IPA without GSH at 25°C (blue triangles, solid line) and 37°C (red circles, solid line) and with GSH at 25°C (blue triangles, dashed line) and 37°C (red circles, dashed line) in aqueous solution of 20 mM GSH.

3.7.2 CUR release profile of CUR-encapsulated nanogels

The release of loaded CUR from the nanogels, initially prepared by PPFMA₄₆-co-POEGMAM₅₄, was monitored by the change of UV absorbance at 425 nm as shown in **Figure 3.13**. As high as 72% of CUR was released after 95 h in the presence of GSH, while there was approximately 36% of released CUR in the absence of GSH over the same period of time at 37°C. The result can confirm that redox-responsive crosslinker was effective in the presence of reducing agent, GSH.

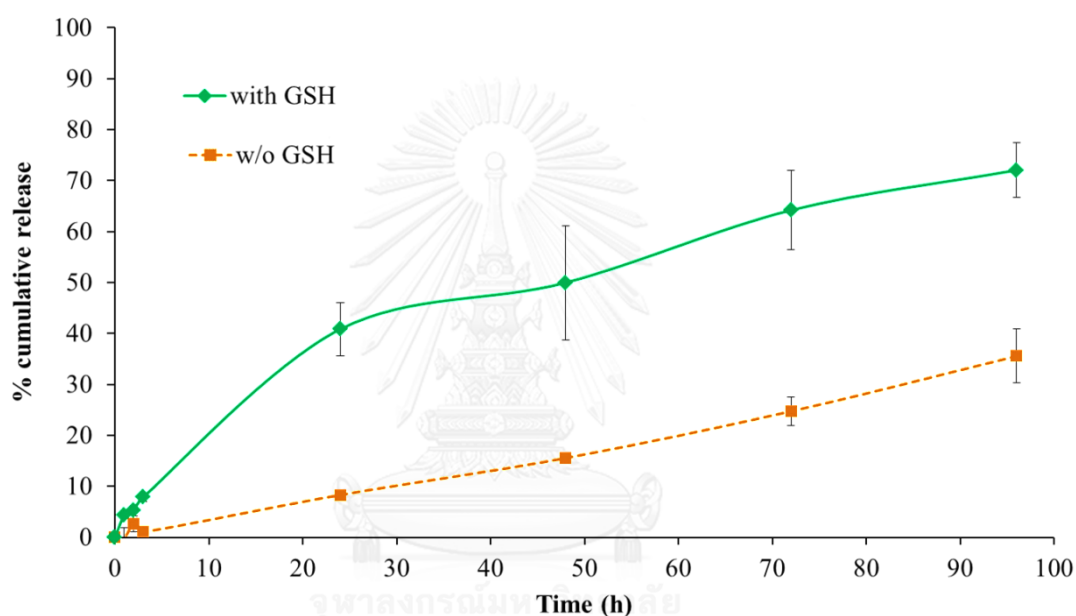


Figure 3.13 CUR release profiles from the CUR-encapsulated nanogels without GSH (orange squares, dashed line) and with GSH (green diamonds, solid line) at 37°C in aqueous solution of 20 mM GSH.

3.8 Cytocompatibility of nanogels

3.8.1 Cytocompatibility against normal cells (L929)

The results from cytocompatibility test against L929 cells shown in **Figure 3.14** suggested that the micelles originally self-assembled from PPFMA₇₃-co-POEGMAM₂₇ became toxic once its concentration is above 0.15 mg/mL (%cell viability < 90%). This detrimental effect comes from the toxic pentafluorophenyl groups being cleaved off from the PFP groups in the copolymer upon hydrolysis

under physiological condition. This speculation can be confirmed by FTIR and ^{19}F NMR analyses. As demonstrated in appendix, the increasing relative intensity between C=O stretching of carboxyl groups at 1721 cm^{-1} and C=O stretching of ester groups at 1780 cm^{-1} implied that greater extent of hydrolysis was induced at 37°C . The release of pentafluorophenyl groups was verified by the emergence of peaks in the ^{19}F NMR spectrum at -164.2 , -165.7 , and -170.9 ppm together with the signals of PFP groups in the copolymer. Since the PFP groups were consumed upon crosslinking, the nanogels became much less toxic as opposed to their original uncrosslinked micelles. %Cell viability remained slightly above 90% in a concentration range of $0.016 - 2\text{ mg/mL}$. As previously demonstrated by FTIR and ^{19}F NMR analyses (**Figure 3.9**), the remaining PFP groups which is the cause of toxicity were almost entirely removed after post-functionalization with IPA. For this reason, the resulting nanogels were essentially non-toxic with 100% cell viability for the concentration up to 2 mg/mL . These tests truly signify the potential of the developed nanogels for biomedical-related applications.

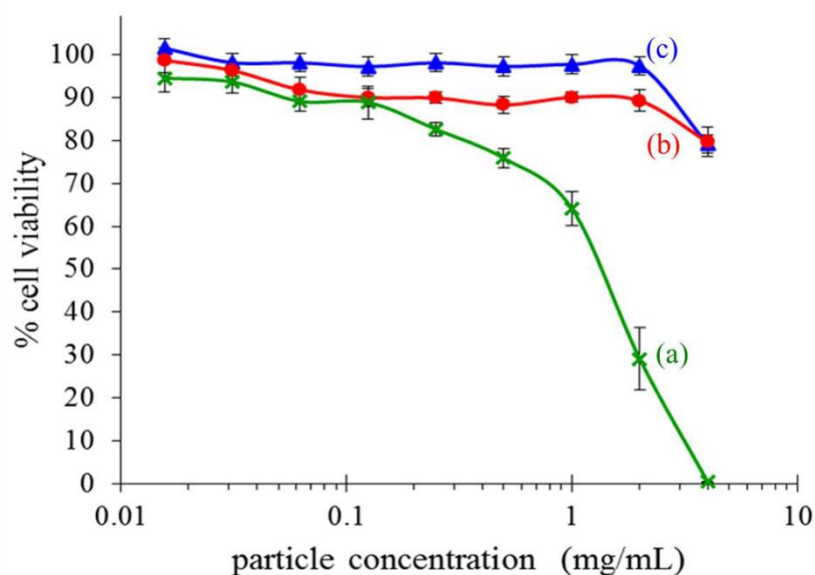


Figure 3.14 Percentage of cell viability of L929 cells after incubation for 24 h with micelles (a), nanogels before (b) and after (c) post functionalized with IPA as determined by MTT assay.

3.8.2 Cytocompatibility against cancer cells (MDA-MB-231)

MDA-MB-231 cells (mammary gland adenocarcinoma cells) as model for cancer cells were treated with CUR, CUR-loaded nanogel and nanogel suspension at equivalent concentrations of CUR and polymer for 24 h, followed by cell viability measurements using MTS assay. We expected that bare nanogel should be biocompatible and free CUR and CUR-loaded nanogel should be toxic against the cells. However, the results (**Figure 3.15**) display that CUR, CUR-loaded nanogel and nanogel are not toxic for the cells in all concentration range of 0.039 - 10 mg/mL (%cell viability > 95%). Although these nanogels were not modified as same as IPA-modified nanogels as previously mentioned, they are still biocompatible. That means crosslinking can effectively eliminate toxic pentafluorophenyl groups of the nanogels. However, both free CUR and loaded CUR in the nanogels had not exhibited their toxicity to the cancer cells. It may be because this range of concentration is too low that the therapeutic activity of CUR cannot affect the cells.

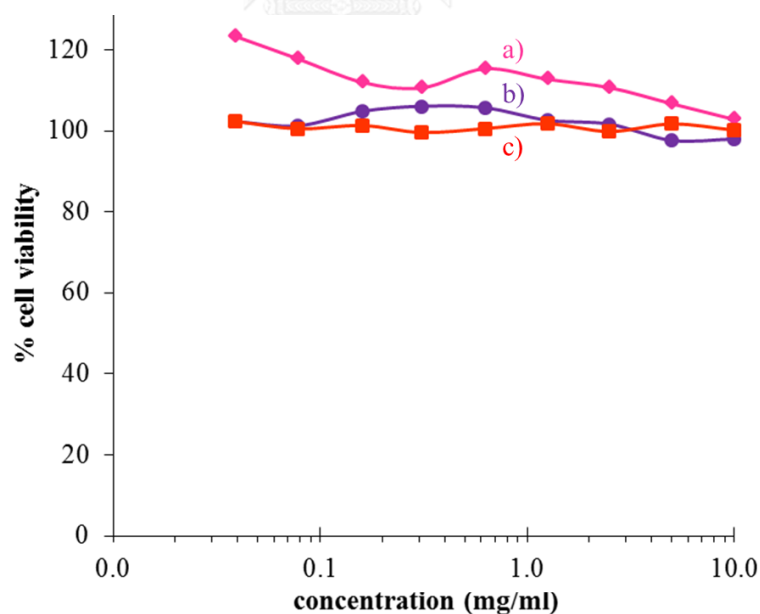


Figure 3.15 Percentage of cell viability of MDA-MB-231 cells after incubation for 24 h with nanogels (a), CUR-loaded nanogels (b) and CUR (c) as determined by MTS assay.

3.9 Cellular Uptake Study

According to luminescent property of CUR, intracellular distribution of CUR can be followed by confocal laser scanning microscopy (CLSM). MDA-MB-231 nuclei were stained with DAPI. Free CUR and CUR-loaded nanogels were administered to the MDA-MB-231 cells and treated for 4 h before fixing them to study their uptake. **Figure3.16** demonstrated that CUR formulation was successfully taken up by MDA-MB-231 cells. A green fluorescent emission of CUR derived from CUR-loaded nanogels were observed in the cytoplasm and the nuclei of the tumor cells as seen in the image of free CUR. This can be implied that the CUR-loaded nanogels can penetrate the cells within a period of 4 h and redox-responsive crosslinkers of the nanogels can degrade in intracellular GSH condition, accelerating the release of CUR from the nanogels. Moreover, the merged images of free CUR and CUR-nanogels show the green fluorescence were overlapped with the blue DAPI-stained nucleus which can be seen as slight cyan in the overlay image, suggesting that the concentration of both free CUR and loaded CUR in the nanogels should be increased to make the images be more obvious.

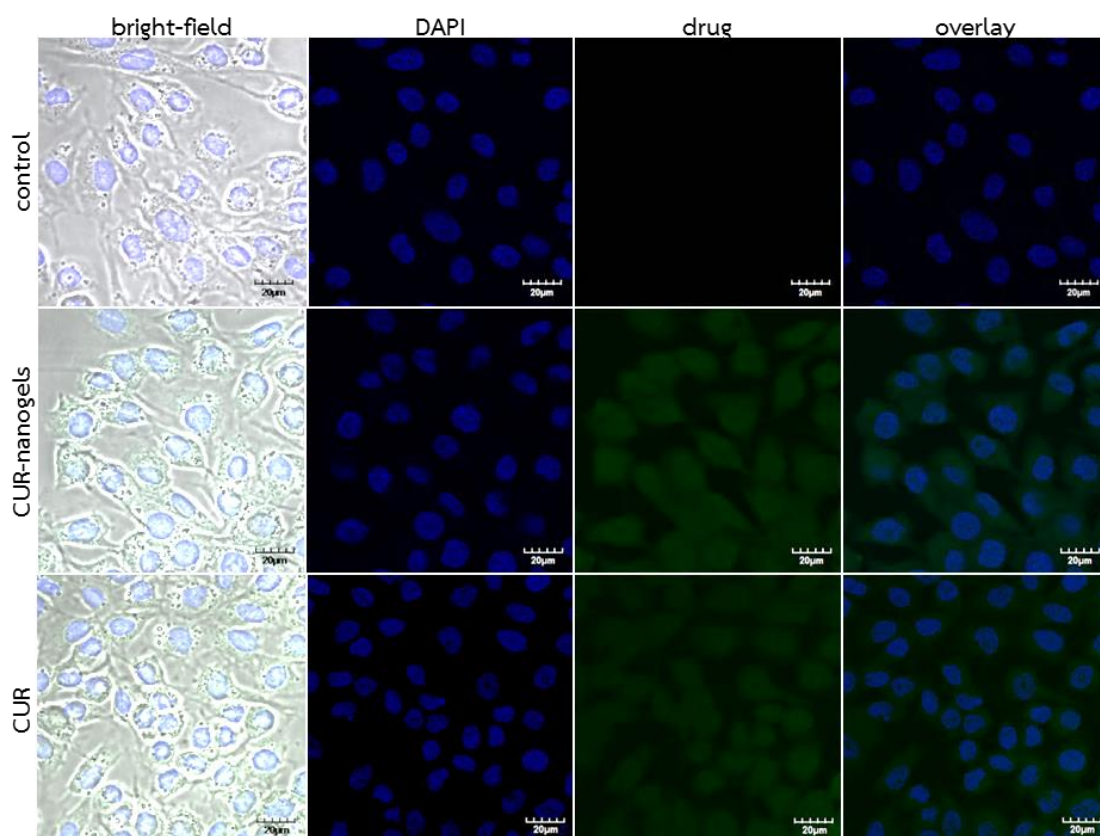


Figure 3.16 CLSM images of MDA-MB-231 cells incubated with free CUR and CUR-loaded nanogels having 10 mg/mL of CUR for 4 h. (blue fluorescence: nucleus staining dye, DAPI; green fluorescence: CUR; scale bar = 20 μm)

CHAPTER IV

CONCLUSION AND SUGGESTION

Amphiphilic copolymers containing PFPMA and OEG can be successfully prepared by post-polymerization modification of PFPMA by OEG-NH₂ with well-defined composition. As verified by DLS and TEM, the nanoparticles formed upon water-induced micellization were spherical in shape and had diameters in the range below 100 nm. Redox-responsive degradation of the nanogels formed after crosslinking the nanoassembled micelles with cystamine was evaluated by DLS. The redox-responsive release of model hydrophobic drug, NR concurrently encapsulated during micellar self-assembly from the nanogels can be realized in the presence of GSH. As high as 94% cumulative NR release was detected at 37°C. Post functionalization of the nanogels with IPA was found to be essential to suppress the release of toxic PFP groups which can be induced by hydrolysis under physiological condition. The fact that there was no NR release at 25°C, w/o GSH implies that the nanogels should maintain their stability upon storage at ambient condition. This information is useful from application viewpoint. In case of CUR release, 72% of CUR can be released in the presence of GSH that is a two-fold increase comparing with the CUR release without GSH.

The cytocompatibility evaluation (MTT assay) indicated that the nanogels post functionalized with IPA were non-toxic in the concentration range of 0.016-2.0 mg/mL. *In vitro* cytotoxicity evaluation by MTS assay suggested that the nanogels were no longer toxic to MDA-MB-231 cells but free CUR and CUR-loaded nanogels were also non-toxic. This is because of too low concentration of CUR-loaded nanogels incubated with the cells. However, CUR-loaded nanogels can penetrate the cells as monitored by CLSM.

Apparently, this research has demonstrated that biocompatible nanogels having enormous potential for controlled-delivery applications can be conveniently

and effectively developed from a single active-ester containing polymer by sequential post-polymerization modification.

From the results of this work, it is suggested that CUR in higher doses (10-100 mg/mL) or other anticancer drugs should be incorporated in this nanogel system, with the hope to develop a more effective controlled release carrier for cancer therapy.



REFERENCES

- [1] Allen TM, Cullis PR. Drug Delivery Systems: Entering the Mainstream. *Science* 2004;303:1818-22.
- [2] Chen W, Zheng M, Meng F, Cheng R, Deng C, Feijen J, et al. In Situ Forming Reduction-Sensitive Degradable Nanogels for Facile Loading and Triggered Intracellular Release of Proteins. *Biomacromolecules* 2013;14:1214-22.
- [3] Farokhzad OC, Langer R. Impact of Nanotechnology on Drug Delivery. *ACS Nano* 2009;3:16-20.
- [4] O'Reilly RK, Hawker CJ, Wooley KL. Cross-linked block copolymer micelles: functional nanostructures of great potential and versatility. *Chemical Society Reviews* 2006;35:1068-83.
- [5] Wooley KL. Shell crosslinked polymer assemblies: Nanoscale constructs inspired from biological systems. *Journal of Polymer Science Part A: Polymer Chemistry* 2000;38:1397-407.
- [6] Ge Z, Liu S. Functional block copolymer assemblies responsive to tumor and intracellular microenvironments for site-specific drug delivery and enhanced imaging performance. *Chemical Society Reviews* 2013;42:7289-325.
- [7] Kim H-C, Park S-M, Hinsberg WD. Block Copolymer Based Nanostructures: Materials, Processes, and Applications to Electronics. *Chemical Reviews* 2010;110:146-77.
- [8] Kim JK, Yang SY, Lee Y, Kim Y. Functional nanomaterials based on block copolymer self-assembly. *Progress in Polymer Science* 2010;35:1325-49.
- [9] Mai Y, Eisenberg A. Self-assembly of block copolymers. *Chemical Society Reviews* 2012;41:5969-85.

- [10] Das A, Theato P. Activated Ester Containing Polymers: Opportunities and Challenges for the Design of Functional Macromolecules. *Chemical Reviews* 2016;116:1434-95.
- [11] Eberhardt M, Théato P. RAFT Polymerization of Pentafluorophenyl Methacrylate: Preparation of Reactive Linear Diblock Copolymers. *Macromolecular Rapid Communications* 2005;26:1488-93.
- [12] Theato P. Synthesis of well-defined polymeric activated esters. *Journal of Polymer Science Part A: Polymer Chemistry* 2008;46:6677-87.
- [13] Eberhardt M, Mruk R, Zentel R, Théato P. Synthesis of pentafluorophenyl(meth)acrylate polymers: New precursor polymers for the synthesis of multifunctional materials. *European Polymer Journal* 2005;41:1569-75.
- [14] Chua GBH, Roth PJ, Duong HTT, Davis TP, Lowe AB. Synthesis and Thermoresponsive Solution Properties of Poly[oligo(ethylene glycol) (meth)acrylamide]s: Biocompatible PEG Analogues. *Macromolecules* 2012;45:1362-74.
- [15] Zhuang J, Jiwpanich S, Deepak VD, Thayumanavan S. Facile Preparation of Nanogels Using Activated Ester Containing Polymers. *ACS Macro Letters* 2012;1:175-9.
- [16] Li Y, Duong HTT, Jones MW, Basuki JS, Hu J, Boyer C, et al. Selective Postmodification of Copolymer Backbones Bearing Different Activated Esters with Disparate Reactivities. *ACS Macro Letters* 2013;2:912-7.
- [17] Allmeroth M, Moderegger D, Biesalski B, Koynov K, Rösch F, Thews O, et al. Modifying the Body Distribution of HPMA-Based Copolymers by Molecular Weight and Aggregate Formation. *Biomacromolecules* 2011;12:2841-9.
- [18] Moad G, Rizzardo E, Thang SH. Radical addition–fragmentation chemistry in polymer synthesis. *Polymer* 2008;49:1079-131.

- [19] Graisuwan W, Zhao H, Kiatkamjornwong S, Theato P, Hoven VP. Formation of thermo-sensitive and cross-linkable micelles by self-assembly of poly(pentafluorophenyl acrylate)-containing block copolymer. *Journal of Polymer Science Part A: Polymer Chemistry* 2015;53:1103-13.
- [20] Jochum FD, Theato P. Temperature- and Light-Responsive Polyacrylamides Prepared by a Double Polymer Analogous Reaction of Activated Ester Polymers. *Macromolecules* 2009;42:5941-5.
- [21] McRae Page S, Martorella M, Parekar S, Kosif I, Emrick T. Disulfide Cross-Linked Phosphorylcholine Micelles for Triggered Release of Camptothecin. *Molecular Pharmaceutics* 2013;10:2684-92.
- [22] Yang F, Cao Z, Wang G. Micellar assembly of a photo- and temperature-responsive amphiphilic block copolymer for controlled release. *Polym Chem* 2015;6:7995-8002.
- [23] Glavas L, Olsén P, Odelius K, Albertsson A-C. Achieving Micelle Control through Core Crystallinity. *Biomacromolecules* 2013;14:4150-6.
- [24] Bapat AP, Ray JG, Savin DA, Sumerlin BS. Redox-Responsive Dynamic-Covalent Assemblies: Stars and Miktoarm Stars. *Macromolecules* 2013;46:2188-98.
- [25] Khorsand B, Lapointe G, Brett C, Oh JK. Intracellular Drug Delivery Nanocarriers of Glutathione-Responsive Degradable Block Copolymers Having Pendant Disulfide Linkages. *Biomacromolecules* 2013;14:2103-11.
- [26] Kim H-C, Kim E, Ha T-L, Jeong SW, Lee SG, Lee SJ, et al. Thiol-responsive gemini poly(ethylene glycol)-poly(lactide) with a cystine disulfide spacer as an intracellular drug delivery nanocarrier. *Colloids and Surfaces B: Biointerfaces* 2015;127:206-12.
- [27] Samarajeewa S, Shrestha R, Elsabahy M, Karwa A, Li A, Zentay RP, et al. In vitro efficacy of paclitaxel-loaded dual-responsive shell cross-linked polymer

nanoparticles having orthogonally degradable disulfide cross-linked corona and polyester core domains. *Molecular Pharmaceutics* 2013;10:1092-9.

[28] Salem M, Rohani S, Gillies ER. Curcumin, a promising anti-cancer therapeutic: a review of its chemical properties, bioactivity and approaches to cancer cell delivery. *RSC Advances* 2014;4:10815-29.





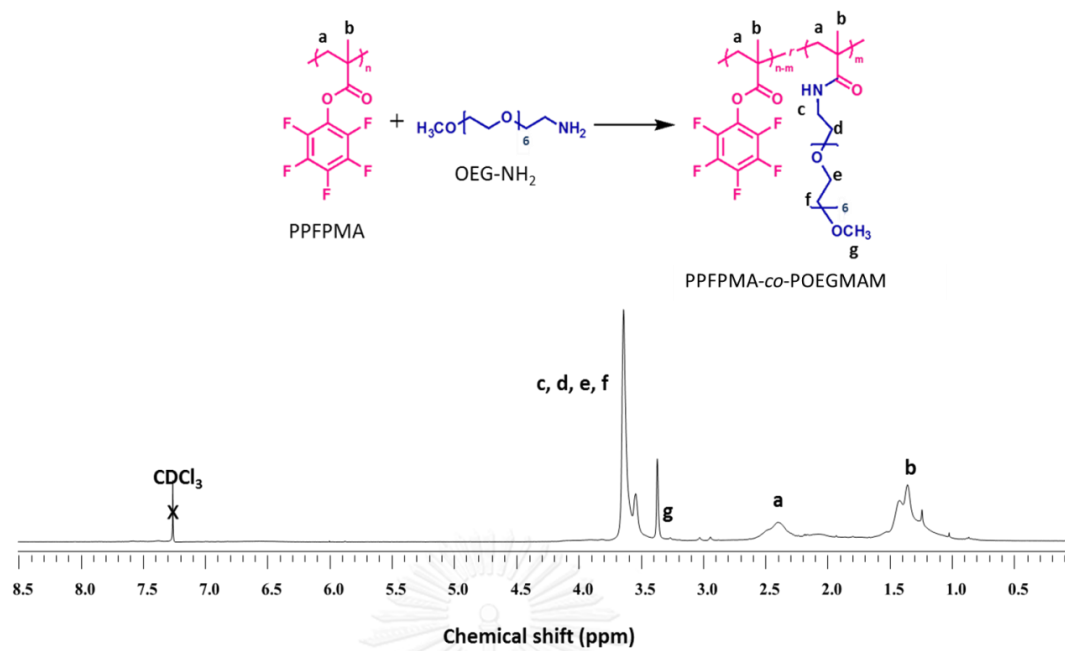


Figure A1 ^1H NMR spectrum of PPFMA₇₃-co-POEGMAM₂₇ in CDCl_3 .

Determination of OEGMAM composition in the amphiphilic copolymer by ^1H NMR

$$\% \text{OEGMAM} = \frac{(\text{integration of peak } g)/3}{(\text{integration of peak } a)/2} \times 100\%$$

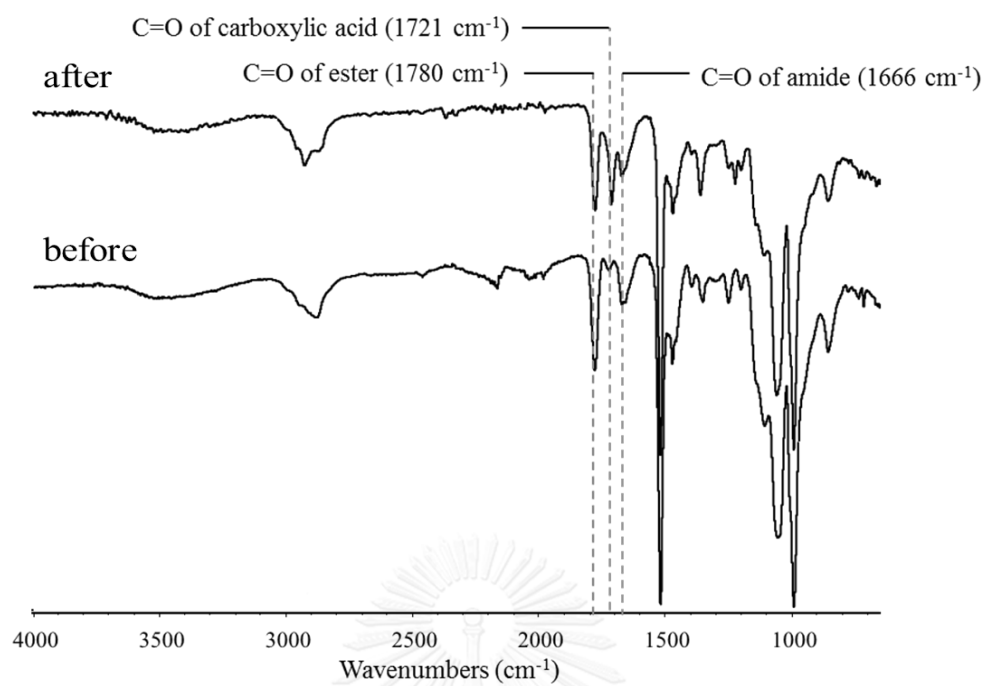


Figure A2 FTIR spectra of PPFMA₇₃-co-POEGMAM₂₇ nanogels before and after induced hydrolysis in PBS at 37°C.

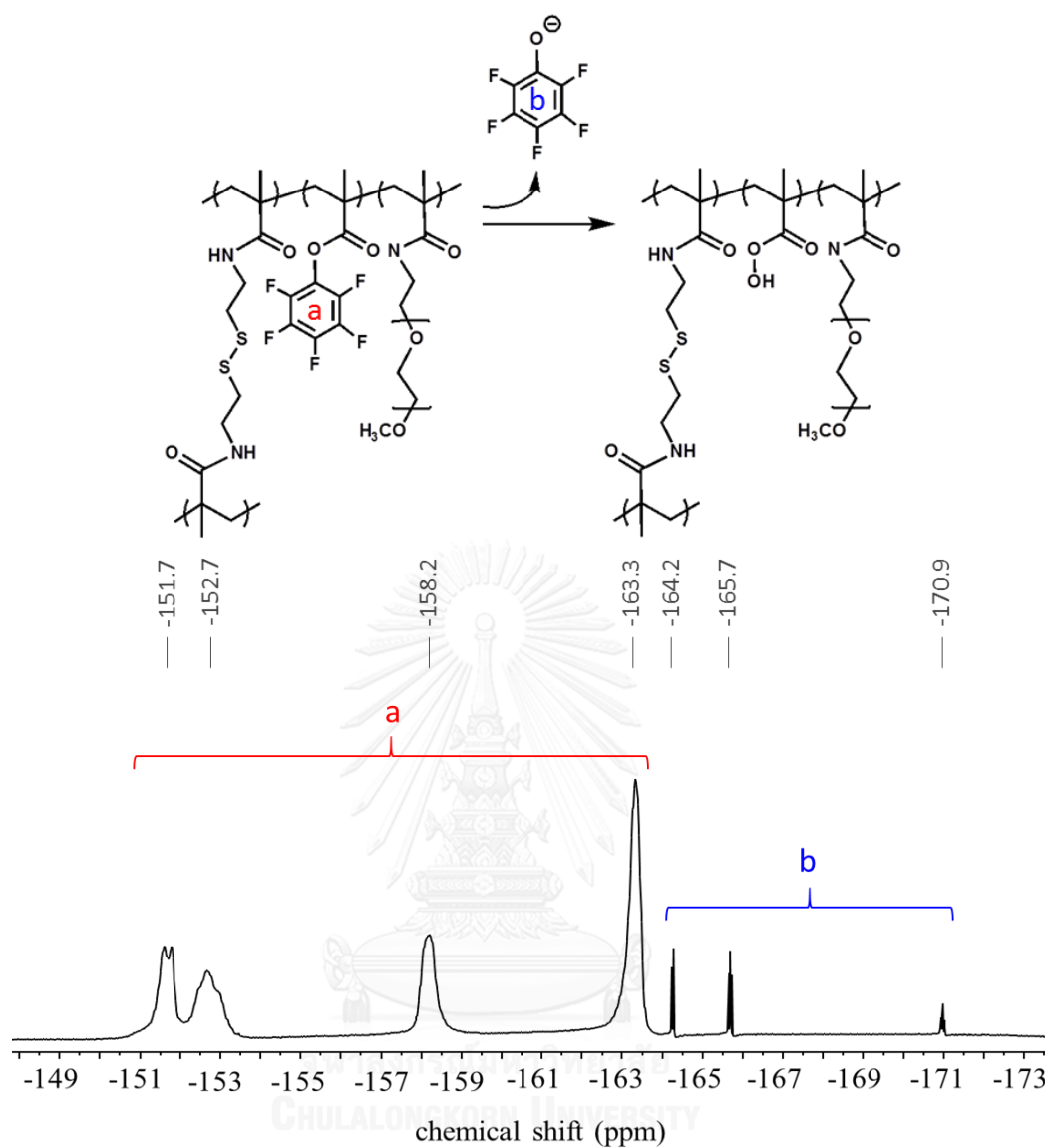


Figure A3 ¹⁹F NMR spectrum of PPFMA₇₃-co-POEGMAM₂₇ nanogels indicating the release of pentafluorophenyl groups after induced hydrolysis in PBS at 37°C.

VITA

Miss Susita Noree was born on May 17th, 1991 in Chachoengsao, Thailand, She received Bachelor Degree of Science in Chemistry from the Faculty of Science, Chulalongkorn University, Bangkok in 2012. In the same year, she started as a Master Degree student with a major in Chemistry, Faculty of Science, Chulalongkorn University and graduated in the academic year of 2016.

Proceeding:

February, 2016; Poster presentation in Polymer Chemistry session at Pure and Applied Chemistry International Conference 2016 (PACCON 2016) at BITEC, Bangkok, Thailand.

Submitted manuscript:

Noree, S.; Tangpasuthadol, V., Hoven V.P. "Cascade Post-Polymerization Modification of Single Pentafluorophenyl ester-bearing Homopolymer as a Facile Route to Redox-responsive Nanogels" Colloid and Interface Science.